Biomedicine & Pharmacotherapy 127 (2020) 110162

Contents lists available at ScienceDirect

Biomedicine & Pharmacotherapy

journal homepage: www.elsevier.com/locate/biopha

Synthesis and trypanocidal activity of novel pyridinyl-1,3,4-thiadiazole derivatives

Rosana H.C.N. Freitas[a,1], Juliana M.C. Barbosa[b,1], Patrícia Bernardino[b], Vitor Sueth-Santiago[c], Solange M.S.V. Wardell[d], James L. Wardell[e], Débora Decoté-Ricardo[f], Tatiana G. Melo[g], Edson F. da Silva[h,i], Kelly Salomão[b,2], Carlos A.M. Fraga[a,*,2]

[a] Laboratório de Avaliação e Síntese de Substâncias Bioativas (LASSBio), Instituto de Ciências Biomédicas, Universidade Federal do Rio de Janeiro, 21941902, Rio de Janeiro, RJ, Brazil
[b] Laboratório de Biologia Celular, Instituto Oswaldo Cruz, Fundação Oswaldo Cruz, 21040-360, Rio de Janeiro, RJ, Brazil
[c] Instituto Federal de Educação, Ciência e Tecnologia do Rio de Janeiro, Campus São Gonçalo, 24425-004, São Gonçalo, RJ, Brazil
[d] CHEMSOL, 1 Harcourt Road, Aberdeen, AB15 5NY, Scotland, UK
[e] Department of Chemistry, University of Aberdeen, Old Aberdeen, AB 24 3 UE, Scotland, UK
[f] Departamento de Microbiologia e Imunologia Veterinária, Instituto de Veterinária, Universidade Federal Rural do Rio de Janeiro, 23890-000, Seropédica, RJ, Brazil
[g] Laboratório de Ultraestrutura Celular, Instituto Oswaldo Cruz, Fundação Oswaldo Cruz, 21040-360, Rio de Janeiro, RJ, Brazil
[h] Instituto de Tecnologia em Fármacos e Farmanguinhos, Fundação Oswaldo Cruz, 21041-250, Rio de Janeiro, RJ, Brazil
[i] Escola de Ciência e Tecnologia, Universidade do Grande Rio, 25071-202, Duque de Caxias, RJ, Brazil

ARTICLE INFO

Keywords:
Chagas disease
Trypanocidal activity
Inhibitor of sterol biosynthesis
2-amino-1,3,4-thiadiazole
1,3,4-thiadiazole-*N*-arylhydrazone

ABSTRACT

Herein, we present the design, synthesis and trypanocidal evaluation of sixteen new 1,3,4-thiadiazole derivatives from *N*-aminobenzyl or *N*-arylhydrazone series. All derivatives were assayed against the trypomastigote form of *Trypanosoma cruzi*, showing IC_{50} values ranging from 3 to 226 μM, and a better trypanocidal profile was demonstrated for the 1,3,4-thiadiazole-*N*-arylhydrazones (**3a-g**). In this series, the 2-pyridinyl fragment bound to the imine subunit of the hydrazine moiety presented pharmacophoric behavior for trypanocidal activity. Compounds **2a**, **11a** and **3e** presented remarkable activity and excellent selectivity indexes. Compound **2a** was also active against the intracellular amastigote form of *T. cruzi*. Moreover, its corresponding hydrochloride, compound **11a**, showed the most promising profile, producing phenotypic changes similar to those caused by posaconazole, a well-known inhibitor of sterol biosynthesis. Thus, 1,3,4-thiadiazole derivative **11a** could be considered a good prototype for the development of new drug candidates for Chagas disease therapy.

1. Introduction

Chagas disease, also known as American trypanosomiasis, is caused by the flagellate protozoan *Trypanosoma cruzi*. The disease was discovered in 1909 and is currently considered by the World Health Organization (WHO) as one of the twenty neglected tropical diseases, affecting more than 5 million people worldwide [1,2]. Even 110 after years its discovery, the etiological treatment for Chagas disease is restricted to two nitroheterocyclic drugs: benznidazole (Bz) and nifurtimox (Nif) (Fig. 1**A**) [3]. Their effectiveness varies with the phase of the infection, dose, period of treatment, and age and geographical origin of the patient [4]. Severe adverse reactions and limited efficacy in the chronic phase justify the need for new drugs/combinations for the treatment of Chagas disease [5]. Thus, intensive research programs have focused on the search for alternative natural or synthetic lead trypanocidal compounds for drug development.

Currently, two approaches are commonly used in the development of drugs for neglected diseases: combination and repositioning [6]. In the context of repositioning, inhibitors of the biosynthetic pathway of ergosterol, originally developed against fungi, are being intensively investigated for pathogenic trypanosomatids. Like fungi, *T. cruzi* has a strict requirement for specific endogenous ergosterol, and for this reason, enzymes of sterol metabolism have been intensively studied as drug targets [7]. C14-α-sterol demethylase of *T. cruzi* (TcCYP51) is a key enzyme for the biosynthesis of ergosterol, catalyzing the removal of the C14 methyl group of lanosterol [8,9]. The majority of CYP51

* Corresponding author at: Centro de Ciências da Saúde, Av. Carlos Chagas Filho, 373, PO Box 68023, Ilha do Fundão, 21941-971, Rio de Janeiro, RJ, Brazil.
E-mail address: cmfraga@ccsdecania.ufrj.br (C.A.M. Fraga).
[1] R.H.C.N. Freitas and J.M.C. Barbosa contributed equally to this article.
[2] Both authors contributed equally as senior authors.

https://doi.org/10.1016/j.biopha.2020.110162
Received 25 February 2020; Received in revised form 8 April 2020; Accepted 13 April 2020

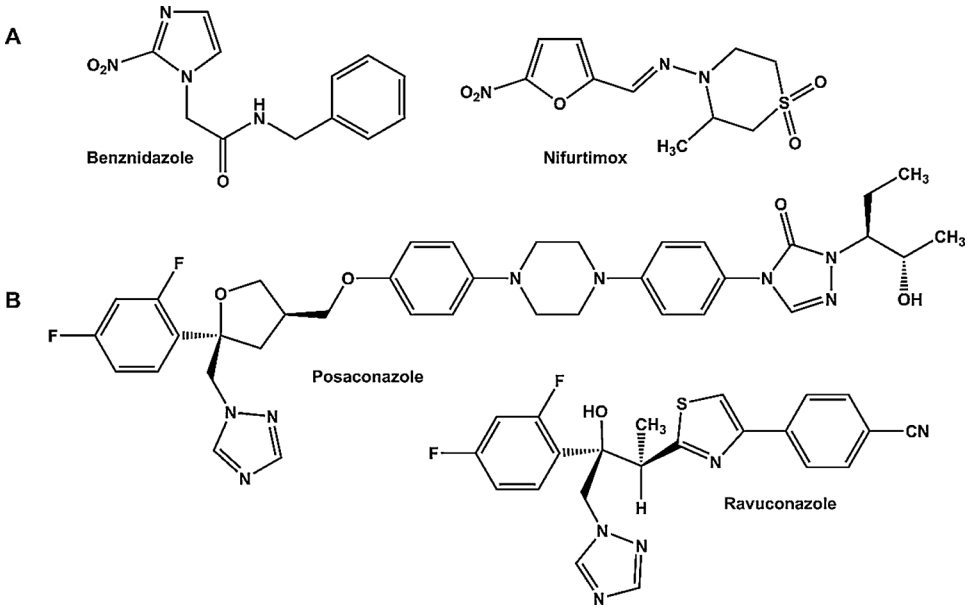

Fig. 1. (A) Drugs employed for the etiological treatment of Chagas disease. (B) Examples of azole TcCYP51 inhibitors.

inhibitor studies involve the repositioning of antifungal azoles. Several azoles at nanomolar concentrations have displayed a strong binding affinity for TcCYP51 and trypanocidal activity, interfering with sterol biosynthesis in intracellular amastigotes, and *in vivo* assays have led to high levels of parasitological cure [10–14]. In phase II clinical trials with chronic patients, monotherapy with both azole compounds posaconazole [15] and ravuconazole (E-1224) [16] (Fig. 1B) failed to maintain a sustained response. Recent results of a phase II clinical trial showed that both monotherapy with Bz and the combination of Bz/E1224 were efficacious [17]. Thus, TcCYP51 inhibition remains a promising target for the development of novel trypanocidal compounds [18].

Among the TcCYP51 inhibitors described in the literature, prototype **1** (Fig. 2) was active at the nanomolar level *in vitro* against intracellular amastigotes with an excellent selectivity index (SI) and high efficacy in mouse models [19]. Since the 3-pyridine moiety of **1** (A, Fig. 2) is considered pharmacophoric for the inhibition of TcCYP51 due to its ability to coordinate with heme iron, we planned a new series of regioisomeric pyridinyl-1,3,4-thiadiazole derivatives **2a-f** (Fig. 2). These compounds were designed by replacing the amide subunit of **1** (B, Fig. 2) with the isosteric 1,3,4-thiadizole ring [20], which has been described as a stable peptidomimetic group [21,22], aiming to prevent the characteristic hydrolytic lability of peptide bonds. Moreover, an azamethylene linker was attached to the heterocyclic subunit in order to mimic the basic behavior of the N-arylpiperazine unit of **1** (C, Fig. 2).

During the structural planning of **2a-f**, a series of molecular simplifications [23] of the auxophoric groups of **1** (E, Fig. 2) were performed. In addition, compounds containing a carbon-fluorine subunit instead of the pharmacophoric aromatic nitrogen of the 4-pyridine ring were also planned, exploiting the well-known isosteric relationship between these groups [20] as represented by retroisosteres **2a** and **2d** (Fig. 2). Finally, a more rigid series of aza-homolog derivatives (**3a-f**) presenting a hydrazone group was also developed (Fig. 3), aiming to better understand the influence of this spacer unit on the trypanocidal activity of these pyridinyl-1,3,4-thiadiazoles. This spacer group was selected in function of the conformational restriction promoted by the presence of conjugated imine double bond and good chemical stability [24], which makes it very attractive for the construction of bioactive compounds of different therapeutic classes [25].

Therefore, in this paper, we describe the synthesis, structural characterization and trypanocidal profile of pyridinyl-1,3,4-thiadiazole

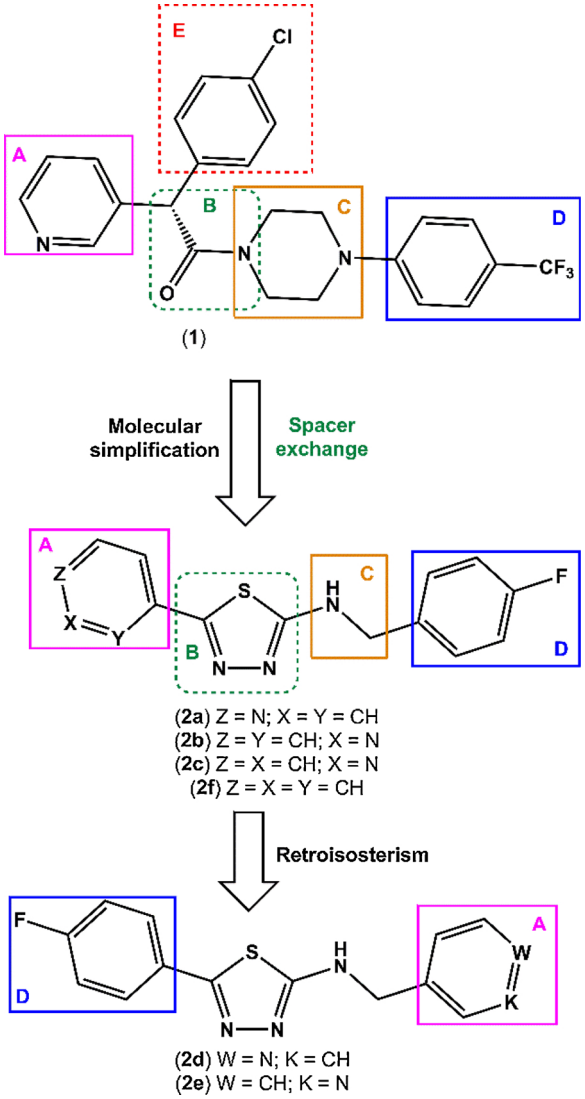

Fig. 2. Design concept of pyridinyl-1,3,4-thiadiazole derivatives **2a-f**.

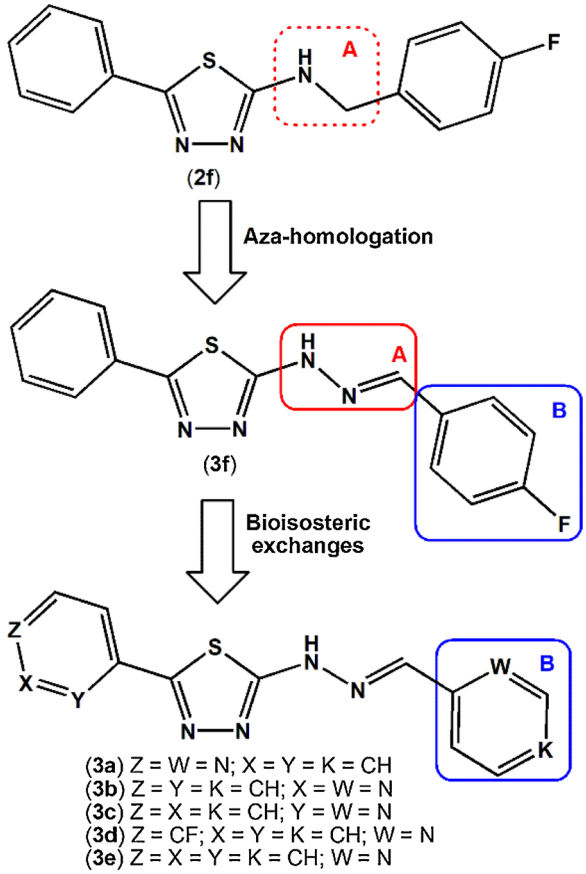

Fig. 3. Design of 1,3,4-thiadiazole-arylhydrazone derivatives **3a-f**.

derivatives **2a-f** and **3a-f** against the clinically relevant forms of *T. cruzi*.

2. Material and methods

2.1. Chemistry

General information: Purification of the products was performed by column chromatography using silica gel (230–400) flash (Merck, Darmstadt) as the stationary phase and mixtures of *N*-hexane and ethyl acetate or dichloromethane and methanol in various proportions as the mobile phase. ^{1}H NMR and ^{13}C NMR were obtained on a Bruker DPX-200 (4.7 T), Bruker DRX-300 (7.05 T), Bruker AVHD400 (9.4 T), or Bruker AVIII500 (11.7 T) spectrometer operating at 200, 300, 400 or 500 MHz, respectively. Chemical shifts (δ) are given in parts per million (ppm) with tetramethylsilane (TMS) as the internal standard and coupling constant (*J*) values are given in Hertz (Hz). The deuterated solvent used to obtain the spectra was dimethyl sulfoxide-d_6 (DMSO-d_6) using NMR-specific glass tubes (5 mm diameter).

Infrared (IR) spectra were obtained in a Nicolet 6700 Fourier transform IR (FT-IR) spectrophotometer apparatus a using potassium bromide pellets.

The chromatographic purity of the final products was determined by HPLC on a Shimadzu LC-20CE apparatus with a Kromasil 100-5 C18 column (4.6 mm × 250 mm) and an SPD-M20A diode array detector. Quantification of the final compounds was performed at a wavelength of 300 nm. The mobile phase used was acetonitrile and water (60–80%), varying the running time between 10 and 20 min.

Melting points were determined on a Quimis Q340.23 apparatus and were not corrected.

Determination of the aqueous solubility was performed using a scanning UV–vis Femto spectrophotometer (model 800XI).

Microanalyses were carried out using a Thermo Scientific Flash EA 1112 series CHN-Analyzer, using a Mettler MX5 electronic balance.

2.1.1. General procedure for the synthesis of methyl esters (5b-e)

To a solution of the respective aryl-carboxylic acid (**4c-e**, 4.09 mmol) in 10 mL methanol was added 15 mL toluene and 3 drops of concentrated sulphuric acid. The obtained mixture was refluxed at 110 °C for 48 h. After that, the solvent was concentrated under reduced pressure and then 10 mL of 10 % aqueous sodium carbonate solution was added to the residue, forming an emulsion. Next, this emulsion was partitioned between dichloromethane (3 × 30 mL) and brine (3 × 30 mL). The organic phases were combined, dried with anhydrous sodium sulphate and evaporated under reduced pressure to furnish the corresponding methyl esters (**5c-e**) [26], as described next. Methyl nicotinate (**5b**) was purchased from Sigma-Aldrich (St. Louis, MO, USA).

2.1.1.1. Methyl picolinate (5c). Compound (**5c**) was obtained in 44 % yield as a colorless oil. ^{1}H NMR (300 MHz, DMSO-d_6) δ (ppm): 3.87 (3H, s, $\underline{CH_3}$), 7.61–7.65 (1H, m), 7.95–8.06 (2H, m), 8.70 (1H, d, J = 6 Hz); ^{13}C NMR (75 MHz, DMSO-d_6) δ (ppm): 52.4 ($\underline{CH_3}$), 124.8 (C3), 127.4 (C5), 137.5 (C4), 147.5 (C2), 149.7 (C6), 165.2 ($\underline{C}$=O); IR (KBr) cm^{-1}: 1249 (C-O), 1585 and 1651 (C = C), 1731 (C = O).

2.1.1.2. Methyl 4-fluorobenzoate (5d). Compound (**5d**) was obtained in 70 % yield as a colorless oil. ^{1}H NMR (300 MHz, DMSO-d_6) δ (ppm): 3.84 (3H, s, $\underline{CH_3}$), 7.34 (2H, t, J = 9 Hz), 7.99–8.04 (2H, m);^{13}C NMR (75 MHz, DMSO-d_6) δ (ppm): 52.3 ($\underline{CH_3}$), 115.9 (C3 and C5), 126.3 (C1), 132.1 (C2 and C6), 163.5 and 166.8 (C4, C-F coupling), 165.4 (C = O); IR (KBr) cm^{-1}: 1278 (C-O), 1582 and 1601 (C = C), 1724 ($\underline{C}$=O).

2.1.1.3. Methyl benzoate (5e). Compound (**5e**) was obtained in 82 % yield as a colorless oil. ^{1}H NMR (300 MHz, DMSO-d_6) δ (ppm): 3.85 (3H, s, $\underline{CH_3}$),7.52 (2H, t, J = 9 Hz), 7.65 (1H, d, J = 9 Hz), 7.96 (2H, d, J = 3 Hz); ^{13}C NMR (75 MHz, DMSO-d_6) δ (ppm): 52.2 ($\underline{CH_3}$), 128.8 (C3 and C5), 129.2 (C2 and C6), 129.7 (C1), 133.3 (C4), 166.3 ($\underline{C}$=O); IR (KBr) cm^{-1}: 1238 and 1281 (C-O), 1509 and 1602 (C = C), 1728 (C = O).

2.1.2. General procedure for the synthesis of hydrazides (6b-e)

To a solution of the methyl ester (**5b-e**, 3.68 mmol) in 20 mL of ethanol was added 2.68 mL of 80 % aqueous hydrazine hydrate (55.2 mmol) and the mixture was refluxed for 6 h. After that, the excess of solvent was removed under reduced pressure and the residue was partitioned between chloroform (3 × 30 mL) and brine (3 × 30 mL).The organic phases were combined, dried with anhydrous sodium sulphate and evaporated under reduced pressure to furnish the corresponding hydrazides (**6b** and **6c**). Alternatively, in the case of the hydrazides **6d** and **6e** a mixture of ice/water was added to promote the formation of precipitates, which were collected by filtration under reduced pressure. The structural characterization and yields of the hydrazides (**6b-6e**) are described next [27].

2.1.2.1. Nicotinylhydrazide (6b). Compound (**6b**)was obtained in 55 % yield as a white solid, mp. 159−160 °C. ^{1}H NMR (500 MHz, DMSO-d_6) δ (ppm): 7.48 (1H, t, J =5 Hz), 8.14 (1H, d, J = 10 Hz), 8.67 (1H, d, J =5 Hz), 8.94 (1H, s), 9.99 (1H, br., NH);^{13}C NMR (125 MHz, DMSO-d_6) δ (ppm): 123.7 (C5), 129.0 (C3), 134.9 (C4), 148.2 (C2), 151.9 (C6), 164.6 (C = O); IR (KBr) cm^{-1}: 1596 (C = C), 1673 (C = O), 3206 and 3323 (N-H).

2.1.2.2. Picolinylhydrazide (6c). Compound (**6c**) was obtained in 50 % yield as a colorless oil. ^{1}H NMR (300 MHz, DMSO-d_6) δ (ppm):4.61 (2H, br., NH_2), 7.52–7.58 (1H, m), 7.94–7.98 (2H, m), 8.6 (1H, d, J =4 Hz), 9.88 (1H, br., NH); ^{13}C NMR (75 MHz, DMSO-d6)δ (ppm): 121.7 (C3), 126.2 (C5), 137.6 (C4), 148.5 (C6), 149.8 (C2), 162.6 (C = O); IR (KBr) cm^{-1}: 1585 and 1651 (C = C), 1731 (C = O), 3433 (N-H).

*2.1.3.1. 4-Fluorobenzoylhydrazide (**6d**).* Compound (**6d**) was obtained in 53 % yield as a white solid, mp. 162 − 164 °C. ^{1}H NMR (300 MHz, DMSO-d_6) δ (ppm): 4.49 (2H, br., NH_2), 7.28 (2H, t, J = 9 Hz), 7.86–7.91 (2H, m), 9.79 (1H, br., NH); ^{13}C NMR (75 MHz, DMSO-d_6) δ (ppm):115.8 (C3 and C5), 130.1 (C2 and C6), 162.6 and 165.9 (C4, C-F coupling), 165.4 (C = O); IR (KBr) cm^{-1}: 1619 (C = C), 1663 (C = O), 3222 and 3303 (N-H).

*2.1.3.2. Benzoylhydrazide (**6e**).* Compound (**6e**) was obtained in 63 % yield as a white solid, mp. 114 − 115 °C. ^{1}H NMR (300 MHz, DMSO-d_6) δ (ppm): 4.53 (2H, br., NH_2), 7,42-7,53 (3H, m), 7.82–7.84 (2H, d, J = 6 Hz), 9. (1H, br., NH); ^{13}C NMR (75 MHz, DMSO-d_6) δ (ppm): 127.2 (C2 and C6), 128.6 (C3 and C5), 131,3 (C4), 133.6 (C1), 166.2 (C = O); IR (KBr) cm^{-1}: 1579 e 1616 (C = C), 1662 (C = O), 3197 and 3300 (N-H).

*2.1.4. Synthesis of 2-amino-1,3,4-thiadiazoles (**7b-e**)*

To a solution of the corresponding hydrazide (**6b-e**, 4 mmol) in 20 mL of ethanol equimolar amount of trimethylsilylisothiocyanate (TMSNCS) was added. The resulting mixture was refluxed at 80 °C for 4 h. Subsequently, the solvent was reduced at reduced pressure, resulting in the formation of a solid mass that was collected by filtration on a Büchner funnel. After drying, these solids were transferred to an Erlenmeyer flask and 3 mL of sulfuric acid was added. This suspension was agitated at room temperature for 12 h. The flask was cooled at 0 °C with an ice bath and a mixture of ice and water was added, increasing the temperature and promoting gas release. After cooling, the precipitate obtained was filtered at reduced pressure on Büchner for the isolation of the 2-amino-1,3,4-thiadiazoles **7d** and **7e**. For the 2-amino-1,3,4-thiadiazoles **7b** and **7c**, it was necessary to increase the pH to 8 using ammonium hydroxide and maintain the mixture at 0 °C. The solid formed was filtered on a Büchner funnel and the compounds **7b-c** were obtained as described next [28]. 5-(Pyridin-4-yl)-1,3,4-thiadiazol-2-amine (**7a**) was purchased from Sigma-Aldrich.

*2.1.4.1. 5-(Pyridin-3-yl)-1,3,4-thiadiazol-2-amine (**7b**).* Compound **7b** was obtained in 52 % yield as a light yellow solid, m.p. 237 − 238 °C.^{1}H NMR (500 MHz, DMSO-d_6) δ (ppm): 7.47–7.51 (1H, m), 7.55 (2H, br, NH_2), 8.13 (1H, dt, J = 10 Hz, J = 5 Hz), 8.61 (1H, dd, J = 5 Hz and J = 5 Hz), 8.94 (1H, s); ^{13}C NMR (125 MHz, DMSO-d_6) δ (ppm): 124.1 (C5' of 3-Py), 127.1 (C3' of 3-Py), 133.5 (C4' of 3-Py), 146.9 (C2' of 3-Py), 150.2 (C6' of 3-Py), 153.3 (C5), 169.1 (C2); IR (KBr) cm-1: 1644 and 1514 (C = C), 3277 (N-H).

*2.1.4.2. 5-(Pyridin-2-yl)-1,3,4-thiadiazol-2-amine (**7c**).* Compound **7c** was obtained in 47 % yield as a light yellow solid, m.p. 263 − 265 °C.^{1}H NMR (300 MHz, DMSO-d_6) δ (ppm): 7.40 (1H, t, J = 4 Hz), 7.51 (2H, br, NH_2), 7.90 (1H, t, J = 8 Hz) 8.04 (1H, d, J = 8 Hz); 8.57 (1H, d, J = 4 Hz); ^{13}C NMR (75 MHz, DMSO-d_6) δ (ppm):119.0 (C3' of 2-Py), 124.2 (C5' of 2-Py), 137.3 (C4' of 2-Py), 149.5 (C6' of 2-Py), 158.5 (C5), 170.0 (C2); IR (KBr) cm^{-1}: 1585 and 1620 (C = C), 3262 (N-H).

*2.1.4.3. 5-(4-Fluorophenyl)-1,3,4-thiadiazol-2-amine (**7d**).* Compound **7d** was obtained in 34 % yield as a grey solid, m.p. 238 − 240 °C.^{1}H NMR (200 MHz, DMSO-d_6) δ (ppm): 7.30 (2H, t, J = 8 Hz), 7.42 (2H, br, NH_2), 7.77–7.83 (2H, m); ^{13}C NMR (75 MHz, DMSO-d_6) δ (ppm):116.7 (C3' and C5' of Ar), 128.1 (C1' of Ar), 129.0 (C2'and C6' of Ar), 155.8 (C5), 160.8 and 165.6 (C4' of Ar, C-F coupling), 169.1 (C2); IR (KBr) cm^{-1}: 1615 and 1516 (C = C), 3338 and 3248 (N-H).

*2.1.4.4. Phenyl-1,3,4-thiadiazol-2-amine (**7e**).* Compound **7e** was obtained in 67 % yield as a white solid, m.p. 223 − 225 °C.^{1}H NMR (300 MHz, DMSO-d_6) δ (ppm): 7.41–7.49 (5H, m, Ph + NH_2), 7.74 (2H, d, J = 6 Hz); ^{13}C NMR (75 MHz, DMSO-d_6) δ (ppm):126.3 (C2' and C6' of Ar), 129.1 (C3' and C5' of Ar), 129.5 (C4' of Ar), 130.9 (C1' of Ar), 156.4 (C5), 168.5 (C2); IR (KBr) cm^{-1}: 1635 and 1685 (C = C), 3257 (N-H).

*2.1.5. General procedure for the synthesis of the 1,3,4-thiadiazole derivatives (**2a-f**)*

In a flask coupled to a reflux condenser were added equimolar amounts of 1,3,4-thiadiazole-amine (**7a-e**, 2.25 mmol), the corresponding aromatic or heteroaromatic aldehyde (**8a-c**, 2.25 mmol), 5 mL of a 25 % solution of zinc chloride in *N*,*N*-dimethylformamide (DMF) and trimethylsilyl-acetate (TMSOAc, 6.75 mmol, 2.5 equivalents). The mixture was refluxed at 100 °C for 12 h, sufficient time to formation of the imine intermediate (observed by TLC). Then, sodium triacetoxyborohydride (4.4 mmol, 1.5 equivalent) was added to the flask and the mixture was stirred at room temperature for 72 h. After this time, 2 mL water and 4 mL saturated sodium carbonate solution were added to the mixture. For derivatives **2a**, **2d** and **2e** precipitates were formed and the final products were obtained by vacuum filtration using a Büchner funnel. However, to obtain **2b** and **2c** it was necessary a partition between chloroform (50 mL) and brine (50 mL). Then, organic phase was dried with anhydrous sodium sulphate and evaporated under reduced pressure. The obtained residue was purified by column chromatography using a gradient mixture of *N*-hexane and ethyl acetate [29].

*2.1.5.1. N-(4-Fluorobenzyl)-5-(pyridin-4-yl)-1,3,4-thiadiazol-2-amine (**2a**).* Compound **2a** was obtained in 95 % yield as a pale yellow solid, m.p. 154 − 155 °C. ^{1}H NMR(200 MHz, DMSO-d_6) δ (ppm): 4.55 (2H, d, J = 6 Hz, CH2), 7.18 (2H, t, J = 8 Hz), 7.40–7.47 (2H, m), 7.69 (2H, d, J = 6 Hz), 8.64 (2H, d, J = 6 Hz), 8.71 (1H, t, J = 6 Hz); ^{13}C NMR (50 MHz, DMSO-d_6) δ (ppm): 47.3 (CH_2), 115.1 (C3'' and C5'' of Ar), 120.2 (C3' and C5' of 4-Py), 129.6 (C2'' and C6'' of Ar), 134.4 (C1'' of Ar), 137.6 (C4' of 4-Py), 150.5 (C2' and C6' of 4-Py), 154.0 (C5), 159.0 and 163.8 (C4'' of Ar, C-F coupling), 169.4 (C2);IR (KBr) cm^{-1}: 1603 and 1542 (C = C), 3217 (N-H). HPLC purity (λ 300 nm): 98.69 %. Anal. Calcd for $C_{14}H_{11}FN_4S$: C, 58.73; H, 3.87; N, 19.57. Found: C, 58.85; H, 3.86; N, 19.51.

*2.1.5.2. N-(4-Fluorobenzyl)-5-(pyridin-3-yl)-1,3,4-thiadiazol-2-amine (**2b**).* Compound **2b** was obtained as a yellow solid in 33 % yield, m.p. 162 − 164 °C. ^{1}H NMR (300 MHz, DMSO-d_6) δ (ppm): 4.54 (2H, d, J = 3 Hz, CH_2), 7.18 (2H, t, J = 9 Hz), 7.42 (2H, t, J = 9 Hz), 7.48–7.52 (1H, m), 8.12 (1H, d, J = 9 Hz), 8.61–8.64 (2H, m, 3-Py-H + NH), 8.93 (1H, s). ^{13}C NMR (75 MHz, DMSO-d_6) δ (ppm): 47.3 (CH_2), 115.2 (C3'' and C5'' of Ar), 124.3 (C5' of 3-Py), 127.0 (C3' of 3-Py), 129.7 (C2'' and C6''), 133.7 (C4' of 3-Py), 134.7 (C1'' of Ar), 147.0 (C2' of 3-Py), 150.4 (C6' of 3-Py), 153.4 (C5), 159.8 and 163.1 (C4'' of Ar), 168.9 (C2); IR (KBr) cm^{-1}: 1555 and 1509 (C = C), 3177 (N-H). HPLC purity (λ 300 nm): 97.31 %. Anal. Calcd for $C_{14}H_{11}FN_4S$: C, 58.73; H, 3.87; N, 19.57. Found: C, 58.70; H, 3.88; N, 19.62.

*2.1.5.3. N-(4-Fluorobenzyl)-5-(pyridin-2-yl)-1,3,4-thiadiazol-2-amine (**2c**).* Compound **2c** was obtained as a yellow solid in 11 % yield, m.p. 131 − 133 °C. ^{1}H NMR (400 MHz, DMSO-d_6) δ (ppm): 4.52 (2H, d, J = 4 Hz, CH_2), 7.18 (2H, t, J = 8 Hz), 7.40–7.44 (3H, m), 7.90 (1H, t, J = 8 Hz), 8.04 (1H, d, J = 8 Hz), 8.57 (2H, s, 2-Py-H + NH). ^{13}C NMR (100 MHz, DMSO-d_6) δ (ppm): 47.3 (CH_2), 115.1 (C3'' and C5'' of Ar), 119.1 (C3' of 2-Py), 124.4 (C5' of 2-Py), 129.6 (C2'' and C6'' of Ar), 134.6 (C1'' of Ar), 137.4 (C4' of 2-Py), 149.3 (C2' of 2-Py), 149.6 (C6' of 2-Py), 158.5 (C5), 160.2 and 162.6 (C4'' of Ar, C-F coupling), 169.8 (C2); IR (KBr) cm^{-1}: 1603 and 1677 (C = C), 3216 (N-H). HPLC purity (λ 300 nm): 98.79 %. Anal. Calcd for $C_{14}H_{11}FN_4S$: C, 58.73; H, 3.87; N, 19.57. Found: C, 58.77; H, 3.88; N, 19.63.

*2.1.5.4. 5-(4-Fluorophenyl)-N-(pyridin-4-ylmethyl)-1,3,4-thiadiazol-2-amine (**2d**).* Compound **2d** was obtained as a pale yellow solid in 53 % yield, m.p. 210 − 212 °C. ^{1}H NMR (200 MHz, DMSO-d_6) δ (ppm): 4.59 (2H, d, J = 2 Hz, CH_2), 7.31 (2H, t, J = 4 Hz), 7.36 (2H, d, J = 2 Hz),

7.78–7.82 (2H, m), 8.53 (2H, d, J = 2 Hz), 8.58 (1H, t, J = 2 Hz, NH).^{13}C NMR (50 MHz, DMSO-d_6) δ (ppm): 46.2 (CH_2), 115.8 (C3' and C5' of Ar), 121.8 (C3" and C5" of 4-Py), 126.9 (C1' of Ar), 128.1 (C2' and C6' of Ar), 147.3 (C4" of 4-Py), 149.1 (C2" and C6" of 4-Py), 155.1 (C5), 159.9 and 164.8 (C4' of Ar, C-F coupling), 167.8 (C2); IR (KBr) cm^{-1}: 1603 and 1502 (C = C), 3191 (N-H). HPLC purity (λ 300 nm): 95.41 %. Anal. Calcd for $C_{14}H_{11}FN_4S$: C, 58.73; H, 3.87; N, 19.57. Found: C, 58.83; H, 3.86; N, 19.52.

*2.1.5.5. 5-(4-Fluorophenyl)-N-(pyridin-3-ylmethyl)-1,3,4-thiadiazol-2-amine (**2e**)*. Compound **2e** was obtained as a dark yellow solid in 75 % yield, m.p. 117 − 119 °C. ^{1}H NMR (300 MHz, DMSO-d_6) δ (ppm): 4.58 (2H, d, J = 6 Hz, CH_2), 7.31 (2H, t, J = 9 Hz), 7.4–7.44 (1H, m), 7.78–7.84 (3H, m), 8.48–8.54 (2H, m, 3-Py-H + NH), 8.61 (1H, s). ^{13}C NMR (50 MHz, DMSO-d_6) δ (ppm): 45.0 (CH_2), 116.2 (C3' and C5' of Ar), 123.9 (C5" of 3-Py), 127.3 (C1' of Ar), 128.6 (C2' and C6' of Ar), 134.6 (C3" of 3-Py), 136.3 (C4" of 3-Py), 148.1 (C2" of 3-Py), 148.6 (C6" of 3-Py), 155.5 (C5), 160.3 and 165.2 (C4' of Ar, C-F coupling), 168.1 (C2); IR (KBr) cm^{-1}: 1669 and 1557 (C = C), 3269 (N-H). HPLC purity (λ 300 nm): 96.82 %. Anal. Calcd for $C_{14}H_{11}FN_4S$: C, 58.73; H, 3.87; N, 19.57. Found: C, 58.90; H, 3.86; N, 19.51.

*2.1.5.6. N-(4-Fluorobenzyl)-5-phenyl-1,3,4-thiadiazol-2-amine (**2f**)*. Compound **2f** was obtained as a beige solid in 39 % yield, m.p. 150 − 152 °C. ^{1}H NMR (300 MHz, DMSO-d_6) δ (ppm): 4.52 (2H, d, J = 6 Hz, CH_2), 7.18 (2H, t, J = 9 Hz), 7.41–7.47 (5H, m), 7.74 (2H, d, J = 9 Hz), 8.47 (1H, t, J = 6 Hz, NH); ^{13}C NMR (50 MHz, DMSO-d_6) δ (ppm): 47.2 (CH_2), 115.1 (C3" and C5" of Ar), 126.3 (C2' and C6' of Ph), 129.1 (C3' and C5' of Ph), 129.5 (C4' of Ph), 129.6 (C2" and C6" of Ar), 130.7 (C1' of Ph), 134.7 (C1" of Ar), 156.3 (C5), 158.9 and 163.7 (C4" of Ar, C-F coupling), 168.2 (C2); IR (KBr) cm^{-1}: 1562 and 1509 (C = C), 3176 (N-H). HPLC purity (λ 300 nm): 95.52 %. Anal. Calcd for $C_{15}H_{12}FN_3S$: C, 63.14; H, 4.24; N, 14.73. Found: C, 63.22; H, 4.25; N, 14.67.

*2.1.6. General procedure for the synthesis of 1,3,4-thiazolyl-chlorides (**9a-e**)*

A solution of corresponding 2-amino-1,3,4-thiadiazole derivative (**7a-e**, 2.81 mmol, 1 equiv.) in a mixture of 7 mL concentrated hydrochloric acid (HCl) and 3 mL water was maintained at 0 °C. Then, sodium nitrite ($NaNO_2$, 14 mmol, 5 equiv.) was added to the flask, resulting in intense gas release and the visual modification of the reaction medium to a strong yellow colour. Then, hydrated copper chloride ($CuCl_2 \cdot 2H_2O$, 14 mmol, 5 equiv.) was added and the solution darkened. The mixture was kept under magnetic stirring at 0 °C for 2 h. Then, still in an ice bath, 4 mL water was added to the reaction medium, followed by neutralization to pH 8 with the addition of ammonium hydroxide. Next, the suspension was extracted with ethyl acetate and saturated NaCl solution. The organic phase was dried with anhydrous sodium sulphate and evaporated under reduced pressure to yield the desired heteroaryl chlorides (**9a-e**). For the derivatives **9d** and **9e**, neutralization and extraction were not necessary. The isolation occurred by adding water and ice to the flask followed by vacuum filtration to collect the precipitates formed [30]. The yields and the careful structural characterization of the 1,3,4-thiadiazolyl-chlorides (**9a-e**) are described next.

*2.1.6.1. 4-(5-Chloro-1,3,4-thiadiazol-2-yl)pyridine (**9a**)*. Compound (**9a**) was obtained as a crystalline solid in 55 % yield. ^{1}H NMR (300 MHz, DMSO-d_6) δ (ppm): 7.92 (2H, d, J = 6 Hz), 8.79 (2H, d, J = 6 Hz); ^{13}C NMR (75 MHz, DMSO-d_6) δ (ppm): 121.2 (C3' and C5' of 4-Py), 135.7 (C6), 150.9 (C2' and C6' of 4-Py), 155.0 (C5), 168.6 (C2); IR (KBr) cm^{-1}: 827 (C-Cl), 1554 and 1593 (C = C).

*2.1.6.2. 3-(5-Chloro-1,3,4-thiadiazol-2-yl)pyridine (**9b**)*. Compound (**9b**) was obtained as a crystalline beige solid in 68 % yield. ^{1}H NMR (300 MHz, DMSO-d_6) δ (ppm): 7.60 − 7.4 (1H, m), 8.34 (1H, d, J = 9 Hz), 8.78 (1H, s), 9.13 (1H, s,); ^{13}C NMR (75 MHz, DMSO-d_6) δ (ppm): 124.1 (C5' of 3-Py), 125.0 (C3' of 3-Py), 134.8 (C4' of 3-Py), 147.8 (C2' of 3-Py), 152.1 (C6' of 3-Py), 153.8 (C5), 167.6 (C2); IR (KBr) cm^{-1}: 823 (C-Cl), 1567 and 1584 (C = C).

*2.1.6.3. 2-(5-Chloro-1,3,4-thiadiazol-2-yl)pyridine (**9c**)*. Compound (**9c**) was obtained as a crystalline light yellow solid in 70 % yield. ^{1}H NMR (300 MHz, DMSO-d_6) δ (ppm): 7.62 (1H, t, J = 6 Hz), 8.05 (1H, t, J = 9 Hz), 8.21 (1H, d, J = 9 Hz), 8.7 (1H, d, J = 6 Hz); ^{13}C NMR (75 MHz, DMSO-d6) δ (ppm): 120.2 (C5' of 2-Py), 126.6 (C4' of 2-Py), 138.2 (C3' of 2-Py), 147.3 (C6' of 2-Py), 150.3 (C2' of 2-Py), 155.3 (C5), 172,6 (C2); IR (KBr) cm^{-1}: 787 (C-Cl), 1567 and 1581 (C = C).

*2.1.6.4. 2-Chloro-5-(4-fluorophenyl)-1,3,4-thiadiazole (**9d**)*. Compound (**9d**) was obtained as an amorphous gray solid in 88 % of yield. ^{1}H NMR (300 MHz, DMSO-d_6) (300 MHz, DMSO-d_6) δ (ppm): 7.42 (2H, t, J = 6 Hz), 7.99–8.04 (2H, m); ^{13}C NMR (75 MHz, DMSO-d_6) δ (ppm): 116.7 (C3' and C5'), 125.5 (C1' of Ar), 130.1 (C2' and C6'), 153.1 (C5), 162.4 and 165.7 (C4' of Ar, C-F coupling), 169.4 (C2); IR (KBr) cm^{-1}: 813 (C-Cl), 1515 and 1600 (C = C).

*2.1.6.5. 2-Chloro-5-phenyl-1,3,4-thiadiazole (**9e**)*. Compound (**9e**) was obtained as an amorphous yellow solid in 71 % yield.^{1}H NMR (300 MHz, DMSO-d_6) δ (ppm): 7.57–7.62 (3H, m), 7.94–7.96 (2H, m); ^{13}C NMR (75 MHz, DMSO-d_6) δ (ppm): 127.5 (C2' and C6'), 128.8 (C4' of Ar), 129.5 (C3' and C5' of Ar), 131.9 (C1' of Ar), 153.1 (C5), 170.5 (C2); IR (KBr) cm^{-1}: 769 (C-Cl), 1427 and 1456 (C = C).

*2.1.7. General procedure for the synthesis of heteroarylhydrazines (**10a-e**)*

To an ethanolic suspension of the heteroaryl chlorides (**9a-e**, 2.03 mmol, 1 equiv.) was added 80 % aqueous hydrazine hydrate (30 mmol, 20 equiv.) at room temperature. Then, the mixture was refluxed at 80 °C for 2 h. After this time, it was possible to observe the total consumption of the starting material and the formation of the desired hydrazine. Then, the solvent was reduced at reduced pressure and an ice/water mixture was added to the resultant residue, promoting immediate precipitation. The solid was collected by filtration on a Büchner funnel to yield the desired heteroarylhydrazine (**10a-e**), as described next [31].

*2.1.7.1. 2-Hydrazinyl-5-(pyridin-4-yl)-1,3,4-thiadiazole (**10a**)*. Compound **10a** was obtained in 81 % yield, as an amorphous beige solid, m.p. 229 − 230 °C. ^{1}H NMR (300 MHz, DMSO-d_6) δ (ppm): 5.25 (2H, br., NH_2), 7.7 (2H, d, J = 9 Hz), 8.63 (2H, d, J = 6 Hz), 9.18 (1H, br, NH); ^{13}C NMR (75 MHz, DMSO-d_6) δ (ppm): 119.9 (C3' and C5' of 4-Py), 138.0 (C4' of 4-Py), 150.4 (C2' and C6' of 4-Py), 154.0 (C5), 178.1 (C2);).IR (KBr) cm^{-1}: 1147 (C-N), 1601 and 1636 (C = C), 3291 and 3310 (N-H).

*2.1.7.2. 2-Hydrazinyl-5-(pyridin-3-yl)-1,3,4-thiadiazole (**10b**)*. Compound **10b** was obtained in 58 % yield, as an amorphous beige solid, m.p. 160 − 161 °C. ^{1}H NMR (300 MHz, DMSO-d_6) δ (ppm): 5.32 (2H, br, NH_2), 7.47–7.51 (1H, m), 8.14 (1H, d, J = 9 Hz), 8.60 (1H, d, J = 3 Hz), 8.95 (1H, s), 9.14 (1H, br, NH); ^{13}C NMR (75 MHz, DMSO-d_6) δ (ppm): 124.1 (C5' of 3-Py), 127.3(C3' of 3-Py), 133.2 (C4' of 3-Py), 146.6 (C2' of 3-Py), 150.1 (C6' of 3-Py), 153.3 (C5), 177.7 (C2); IR (KBr) cm^{-1}: 1153 (C-N), 1586 and 1633 (C = C), 3343 (N-H).

*2.1.7.3. 2-Hydrazinyl-5-(pyridin-2-yl)-1,3,4-thiadiazole (**10c**)*. Compound **10c** was obtained in 67 % yield, as an amorphous yellow solid, m.p. 214 − 216 °C. ^{1}H NMR (400 MHz, DMSO-d_6) δ (ppm): 5.23 (2H, br, NH_2), 7.40(1H, t, J = 6 Hz), 7.89 (1H, t, J = 9 Hz), 8.04 (1H, d, J = 9 Hz), 8.58 (1H, d, J = 6 Hz), 9.11 (1H, br., NH); ^{13}C NMR (75 MHz, DMSO-d_6) δ (ppm):118.7 (C3' of 3-Py), 124.0 (C5' of 3-Py),

137.2 (C4' of 3-Py), 149.5 (C6' of 3-Py), 149.8 (C2' of 3-Py), 158.3 (C5), 178.3 (C2); IR (KBr) cm^{-1}:1139 (C-N), 1587 and 1633 (C = C), 3343 (N-H).

*2.1.7.4. 2-(4-Fluorophenyl)-5-hydrazinyl-1,3,4-thiadiazole (**10d**)*. Compound **10d** was obtained in 63 % yield, as an amorphous beige solid, m.p. 230 − 231 °C. ^{1}H NMR (200 MHz, DMSO-d_6) δ (ppm): 5.22 (2H, br., NH_2), 7.3 (2H, t, J = 6 Hz), 7.79–7.83 (2H, m), 8.97 (1H, br, NH); ^{13}C NMR (75 MHz, DMSO-d_6) δ (ppm): 116.1 (C3' and C5' of Ar), 127.8 (C1' of Ar), 128.2 (C2' and C6' of Ar), 155.3 (C5), 161.3 and 163.8 (C4' of Ar, C-F coupling), 177.3 (C2); IR (KBr) cm^{-1}: 1615 and 1516 (C = C), 3338 and 3248 (N-H).

*2.1.7.5. 2-Hydrazinyl-5-phenyl-1,3,4-thiadiazole (**10e**)*. Compound **10e** was obtained in 67% yield, as an amorphous yellow solid, m.p. 201 − 203 °C. ^{1}H NMR (400 MHz, DMSO-d_6) δ (ppm): 5.21 (2H, br, NH_2), 7.41–7.49 (3H, m), 7.75–7.78 (2H, m), 8.97 (1H, br, NH); ^{13}C NMR (100 MHz, DMSO-d_6) δ (ppm): 126.0 (C3' and C5' of Ar), 129.1 (C2' and C6' of Ar), 129.4 (C4' of Ar), 131.2 (C1' of Ar), 156.4 (C5), 177.1 (C2).IR (KBr) cm^{-1}: 1140 (C-N), 1572 and 1645 (C = C), 3265 (N-H).

*2.1.8. General procedure for the synthesis of 1,3,4-thiadiazolyl-N-arylhydrazone derivatives (**3a-f**)*

Equimolar amounts of heteroaryl-hydrazines (**11a-e**, 1.55 mmol) and 4-fluorbenzaldehyde (**8a**, 1.55 mmol, 1 equiv.) or pyridine-2-carboxaldehyde (8d, 1.55 mmol, 1 equiv.) were added in ethanol in a 50 mL flask. Then, two drops of 10 % HCl were added and after a few minutes it was possible to observe the formation of precipitates in the flask. The mixture was stirred at room temperature for 4 h. After confirming the end of the reaction through the TLC, the solvent volume was reduced in a rotary evaporator and then ice and ice water were added to the flask. Final compounds (**3a-f**) were obtained after vacuum filtration on Büchner funnel [31].

*2.1.8.1. (E)-2-(2-(Pyridin-2-ylmethylene)hydrazinyl)-5-(pyridin-4-yl)-1,3,4-thiadiazole (**3a**)*. Compound **3a** was obtained in 75 % yield, as an amorphous dark yellow solid, m.p. 239 − 240 °C. ^{1}H NMR (400 MHz, DMSO-d_6) δ (ppm): 7.40 (1H, q, J = 4 Hz), 7.84 (2H, d, J = 8 Hz), 7.89 (2H, d, J = 4 Hz), 8.16 (1H, s, imine CH), 8.61 (1H, d, J = 8 Hz), 8.71 (2H, d, J = 4 Hz), 13.01 (1H, br., NH); ^{13}C NMR (100 MHz, DMSO-d_6) δ (ppm): 118.2 (C3'' of 2-Py), 119.0 (C3' and C5' of 4-Py), 120.9 (C5'' of 2-Py), 135.7 (C4'' of 2-Py), 139.7 (C4' of 4-Py), 140.1 (imine CH), 148.0 (C2'' of 2-Py), 148.9 (C6'' of 2-Py), 149.9 (C2' and C6' of 4-Py), 156.4 (C5), 183.4 (C2);IR (KBr) cm^{-1}: 1147 (C-N), 1600 and 1636 (C = C), 3310 (N-H). HPLC purity (λ 300 nm): 99.01 %. Anal. Calcd for $C_{13}H_{10}N_6S$: C, 55.31; H, 3.57; N, 29.77. Found: C, 55.17; H, 3.58; N, 29.87.

*2.1.8.2. (E)-2-(2-(Pyridin-2-ylmethylene)hydrazinyl)-5-(pyridin-3-yl)-1,3,4-thiadiazole (**3b**)*. Compound **3b** was obtained in 79 % yield, as an amorphous yellow solid, m.p. 226 − 227 °C. ^{1}H NMR (400 MHz, DMSO-d_6) δ (ppm): 7.37–7.40 (1H, m, H10), 7.52–7.56 (1H, m), 7.88 (2H, d, J = 4 Hz), 8.12 (1H, s, imine CH), 8.24 (1H, d, J = 8 Hz), 8.60 (1H, d, J = 4 Hz), 8.66 (1H, s), 9.05 (1H, s), 12.9 (1H, br, NH); ^{13}C NMR (100 MHz, DMSO-d_6) δ (ppm): 119.6 (C3'' of 2-Py), 124.0 (C4' of 3-Py), 124.2 (C5'' of 2-Py), 133.7 (C5' of 3-Py), 136.8 (C4'' of 2-Py), 144.5 (imine CH), 147.0 (C2' of 3-Py), 149.5 (C6'' of 2-Py), 150.8 (C6' of 3-Py), 152.7 (C5), 170.0 (C2); IR (KBr) cm^{-1}: 1157 (C-N), 1575 and 1603 (C = C), 3462 (N-H). HPLC purity (λ 300 nm): 97.23 %. Anal. Calcd for $C_{13}H_{10}N_6S$: C, 55.30; H, 3.57; N, 29.77. Found: C, 55.39; H, 3.58; N, 29.65.

*2.1.8.3. (E)-2-(Pyridin-2-yl)-5-(2-(pyridin-2-ylmethylene)hydrazinyl)-1,3,4-thiadiazole (**3c**)*. Compound **3c** was obtained in 81 % yield, as an amorphous yellow solid, m.p. 249 − 250 °C. ^{1}H NMR (400 MHz, DMSO-d_6) δ (ppm): 7.38–7.41 (1H, m), 7.48–7.51 (1H, m), 7.87 (1H, t, J = 8 Hz), 7.92–8.00 (2H, m), 8.11–8.13 (2H, m), 8.60 (1H, d, J = 4 Hz), 8.65 (1H, d, J = 4 Hz), 12.8 (1H, br, NH); ^{13}C NMR (75 MHz, DMSO-d_6) δ (ppm): 119.1 (C3' of 2-Py), 119.5 (C3'' of 2-Py), 124.0 (C5' of 2-Py), 124.8 (C5' of 2-Py), 136.8 (C4' of 2-Py), 137.5 (C4'' of 2-Py), 144.6 (imine CH), 148.9 (C2' of 2-Py), 149.4 (C6' of 2-Py), 149.7 (C6'' of 2-Py), 152.8 (C5), 170.9 (C2); IR (KBr) cm^{-1}: 1159 (C-N), 1564 and 1575 (C = C), 3440 (N-H). HPLC purity (λ 300 nm): 95.48 %. Anal. Calcd for $C_{13}H_{10}N_6S$: C, 55.30; H, 3.57; N, 29.77. Found: C, 55.36; H, 3.57; N, 29.75.

*2.1.8.4. (E)-2-(4-Fluorophenyl)-5-(2-(pyridin-2-ylmethylene)hydrazinyl)-1,3,4-thiadiazole (**3d**)*. Compound **3d** was obtained in 85 % yield, as an amorphous yellow solid, m.p. 243 − 245 °C. ^{1}H NMR (300 MHz, DMSO-d_6) δ (ppm): 7.34–7.37 (3H, m), 7.87 (4H, m), 8.11 (1H, s, imine CH), 8.59 (1H, m), 12.8 (1H, br., NH); ^{13}C NMR (75 MHz, DMSO-d_6) δ (ppm):116.3 (C3' and C5' of Ar), 119.6 (C3'' of 2-Py), 124.0 (C5'' of 2-Py), 127.0 (C1' of Ar), 128.8 (C3' and C5' of Ar), 136.8 (C4'' of 2-Py), 144.5 (C7') 149.5 (C6'' of 2-Py), 152.8 (C5), 161.4 and 164.7 (C4' of Ar, C-F coupling), 169.7 (C2). IR (KBr) cm^{-1}: 1161 (C-N), 1577 and 1600 (C = C), 3201 (N-H). HPLC purity (λ 300 nm): 96.28 %. Anal. Calcd for $C_{14}H_{10}FN_5S$: C, 56.18; H, 3.37; N, 23.40. Found: C, 56.09; H, 3.38; N, 23.46.

*2.1.8.5. (E)-2-Phenyl-5-(2-(pyridin-2-ylmethylene)hydrazinyl)-1,3,4-thiadiazole (**3e**)*. Compound **3e** was obtained in 65 % yield, as an amorphous yellow solid, m.p. 220 − 222 °C. ^{1}H NMR (500 MHz, DMSO-d_6) δ (ppm): 7.38 (1H, m), 7.49–7.51 (3H, m), 7.85–7.88 (4H, m), 8.13 (1H, s, imine CH), 8.59 (1H, m), 12.8 (1H, br., NH); ^{13}C NMR (125 MHz, DMSO-d_6) δ (ppm): 119.6 (C3'' of 2-Py), 124.0 (C5'' of 2-Py), 126.5 (C2' and C6' of Ar), 129.3 (C3' and C5' of Ar), 130.3 (C4' of Ar), 130.4 (C6), 136.9 (C4'' of 2-Py), 144.4 (C2'' of 2-Py), 148.2 (imine CH), 149.5 (C6'' of 2-Py), 152.8 (C5), 169.6 (C2). IR (KBr) cm^{-1}: 1156 (C-N), 1574 and 1601 (C = C), 3481 (N-H). HPLC purity (λ 300 nm): 96.55 %. Anal. Calcd for $C_{14}H_{11}N_5S$: C, 59.77, H, 3.94, N, 24.89. Found: C, 59.91; H, 3.93; N, 24.81.

*2.1.8.6. (E)-2-(2-(4-Fluorobenzylidene)hydrazinyl)-5-phenyl-1,3,4-thiadiazole (**3f**)*. Compound **3f** was obtained in 90 % yield, as an amorphous yellow solid, m.p. 259 − 261 °C. ^{1}H NMR (400 MHz, DMSO-d_6) δ (ppm): 7.28 (2H, t, J = 8 Hz), 7.46–7.53 (3H, m), 7.72–7.75 (2H, m), 7.85 (2H, d, J = 4 Hz) 8.12 (1H, s, imine CH), 12.5 (1H, br., NH); ^{13}C NMR (100 MHz, DMSO-d_6) δ (ppm): 115.9 (C3'' and C5'' of Ar), 126.3 (C2' and C6' of Ar), 128.6 (C2'' and C6'' of Ar), 129.2 (C3' and C5' of Ar), 130.0 (C4' of Ar), 130.5 (C1' of Ar), 130.7 (C1'' of Ar), 143.4 (imine CH), 156.9 (C5), 161.6 and 164.0 (C4'' of Ar, C-F coupling), 169.6 (C2);IR (KBr) cm^{-1}: 1148 (C-N), 1604 and 1621 (C = C), 3445 (N-H). HPLC purity (λ 300 nm): 99.68 %. Anal. Calcd for $C_{15}H_{11}FN_4S$: C, 60.39, H, 3.72; N, 18.78. Found: C, 60.52; H, 3.73; N, 18.71.

*2.1.9. Synthesis of hydrochlorides (**11a-d**)*

Hydrochlorides **11a-d** were obtained in good yields after bubbling hydrochloric acid gas to a solution of corresponding 1,3,4-thiadiazole derivatives **2a**, **2d**, **2e** and **3e** in $CHCl_3$, as previously described [32]. Since hydrochlorides are not new chemical entities, we chose to only characterize these molecules by using ^{1}H NMR and elemental analysis.

*2.1.9.1. N-(4-Fluorobenzyl)-5-(pyridin-4-yl)-1,3,4-thiadiazol-2-amine hydrochloride (**11a**)*. Compound **11a** was obtained in 72 % yield, as an amorphous yellow solid, m.p. 118 − 119 °C. ^{1}H NMR (400 MHz, DMSO-d_6) δ (ppm):4.62 (2H, s), 7.19 (2H, t, J = 8 Hz), 7.42–7.46 (2H, m), 8.27 (2H, d, J = 4 Hz), 8.88 (2H, d, J = 4 Hz), 9.43 (1H, br., NH). Anal. Calcd for $C_{14}H_{12}ClFN_4S$: C, 52.09; H, 3.75; N, 17.36. Found: C, 51.98; H, 3.76; N, 17.41.

*2.1.9.2. 5-(4-Fluorophenyl)-N-(pyridin-4-ylmethyl)-1,3,4-thiadiazol-2-amine hydrochloride (**11b**).* Compound **11b** was obtained in 62 % yield, as an amorphous pale-yellow solid, m.p. 219 − 220 °C. ^{1}H NMR (400 MHz, DMSO-d_6) δ (ppm): 4.92 (2H, s), 7.32 (2H, t, J = 8 Hz), 7.79–7.82 (2H, q), 8.04 (2H, d, J = 4 Hz), 8.89 (2H, d, J = 4 Hz), 9.48 (1H, br, NH). Anal. Calcd for $C_{14}H_{12}ClFN_4S$: C, 52.09; H, 3.75; N, 17.36. Found: C, 52.21; H, 3.74; N, 17.31.

*2.1.9.3. 5-(4-Fluorophenyl)-N-(pyridin-3-ylmethyl)-1,3,4-thiadiazol-2-amine hydrochloride (**11c**).* Compound **11c** was obtained in 98 % yield, as an amorphous dark yellow solid, m.p. 105 − 107 °C. ^{1}H NMR (400 MHz, DMSO-d_6) δ (ppm): 4.76 (2H, s), 7.32 (2H, t, J = 8 Hz), 7.79–7.83 (2H, m), 8.04–8.08 (1H, m), 8.58 (1H, d, J = 8 Hz), 8.85 (2H, d, J = 4 Hz), 8.95 (1H, br., NH). Anal. Calcd for $C_{14}H_{12}ClFN_4S$: C, 52.09; H, 3.75; N, 17.36. Found: C, 51.99; H, 3.74; N, 17.40.

*2.1.9.4. (E)-2-Phenyl-5-(2-(pyridin-2-ylmethylene)hydrazinyl)-1,3,4-thiadiazole hydrochloride (**11d**).* Compound **11d** was obtained in 73 % yield, as an amorphous yellow solid, m.p. 205 − 206 °C. ^{1}H NMR (400 MHz, DMSO-d_6) δ (ppm): 7.50–7.53 (3H, m), 7.59 (1H, t, J = 8 Hz), 7.83–7.86 (2H, m), 8.03 (1H, d, J = 8 Hz), 8.13 (1H, d, J = 8 Hz), 8.22 (1H, s), 8.66 (1H, d, J = 4 Hz). Anal. Calcd for $C_{14}H_{12}ClN_5S$: C, 52.91; H, 3.81; N, 22.04. Found: C, 53.03; H, 3.80; N, 21.99.

2.2. Single crystal X-ray diffraction

After the synthesis and purification procedures, a well-shaped clear single crystal of compound **3d**, was selected for the X-ray diffraction experiment. Atomic coordinates, bond lengths, angles and thermal parameters have been deposited at the Cambridge Crystallographic Data Centre, deposition number CCDC 1968552. Molecules are linked into spiral chains by N1-Hn1—N5 strong hydrogen bonds: also present are weak C18-H188-F1 hydrogen bonds.

2.3. Aqueous solubility determination

Aqueous solubility of some target 1,3,4-thiadiazole derivatives was determined by UV/Vis spectroscopy as described by Schneider et al. [33].

2.4. Biological activity

All experiments dealing with animals were performed in accordance with the Brazilian Law 11.794/2008 and regulations of the National Council of Animal Experimentation Control under the license L038/2018 from the Ethics Committee for Animal Use of the Oswaldo Cruz Institute (CEUA/IOC). The mice were housed at a maximum of 6 individuals per cage, kept in a specific-pathogen-free (SPF) room at 20–22 °C under a 12/12 h light/dark cycle, 50–60% humidity and provided sterilized water and chow *ad libitum*.

2.4.1. In vitro activity of pyridinyl-1,3,4-thiadiazoles against trypomastigotes and intracellular amastigotes of T. cruzi

For all the experiments stock solutions of the 1,3,4-thiadiazole derivatives, ketoconazole, posaconazole and Bz were prepared in dimethyl sulfoxide, with the final concentration of the solvent in the experiments never exceeding 0.6 %, concentration known to exert no toxicity to the parasite or host cells [34]. Bloodstream trypomastigotes of Y strain [35] were obtained from infected Swiss Webster mice at the peak of parasitemia by differential centrifugation. The parasites (5×10^6 cells/mL) were incubated for 24 h at 37 °C and 5% CO_2 atmosphere in absence or presence of the compounds. Cell counts were performed in a Neubauer chamber, by light microscopy and the activity of the compounds was expressed as the IC_{50}/24 h, corresponding to the concentration that led to 50 % lysis of the parasites. The standard drugs ketoconazole, posaconazole and Bz were used as control. The activity of the 1,3,4-thiadiazole derivatives against intracellular amastigote forms of the Y strain was evaluated using primary cultures of mouse embryo heart muscle cells (HMC) as host cells. Briefly, hearts of 18-day-old mouse embryos were fragmented and dissociated with trypsin and collagenase in phosphate-buffered saline (PBS), pH 7.2 and the cells were resuspended in Dulbecco's modified Eagle's medium (Sigma-Aldrich, St. Louis, MO) supplemented with horse and foetal calf serum, chicken embryo extract, $CaCl_2$, and L-glutamine (DMEM) and plated onto gelatine-coated glass coverslips [36]. HMC was infected with bloodstream trypomastigotes (MOI 10:1), and after 24 h of infection, the cells were treated with the compounds. After 24 and 48 h of treatment, the cultures were rinsed with saline, fixed and stained with Diff-Quick Staining (Laborclin), examined by light microscopy and counted and the infection index (II) was determined, this parameter corresponds to the number of parasites/100 cells, obtained by the multiplication of the percentage of infection by the number of parasites/infected cell) [34]. The IC_{50} values for the different days of treatment, corresponding to the concentration that led to 50 % inhibition of this parameter was calculated. Ketoconazole, posaconazole and Bz were used as control.

2.4.2. In vitro toxicity of pyridinyl-1,3,4-thiadiazoles to mammalian cells

Mouse peritoneal macrophages were obtained from Swiss mice, and for the cytotoxicity assays, 2.5×10^4 cells in 200 µL RPMI-1640 medium (pH 7.2, plus 10 % foetal bovine serum (FBS) and 2 mM *L*-glutamine) were added to each well of a 96-well microliter plate and incubated with the 1,3,4-thiadiazole derivatives for 24 h at 37 °C. For the assays with HMC, the cells were plated at the concentration of 5×10^4 in 200 µL in DMEM and treated with the compounds for 24 and 48 h at 37 °C [37]. For both mammalian cells, after treatment, PrestoBlue (Invitrogen) was added in the proportion 1:10, and the microplates were incubated for 2 h and the fluorescence measured at 560 and 590 nm, as recommended by the manufacturer. The results were expressed as the difference in the percentage of reduction between treated and untreated cells being LC_{50} the concentration that leads to damage of 50 % of the mammalian cells [38]. The selectivity index (SI) was calculated by the ratio between LC_{50} and IC_{50} at 24 h for peritoneal macrophages, in experiments with bloodstream trypomastigotes and at both 24 and 48 h for HMC, in experiments with intracellular amastigotes.

2.4.3. Transmission and scanning electron microscopy analysis

Trypomastigotes (Y strain, 5×10^6 cells/mL) were treated for 24 h with the selected compound sat the concentrations corresponding to the IC_{50}/24 h and 2x IC_{50}/24 h values. Afterward, they were fixed with 2.5 % glutaraldehyde in 0.1 M Na-cacodylate buffer (pH 7.2) for 40 min at 25 °C and post-fixed with 1% OsO_4, 0.8 % potassium ferricyanide and 2.5 mM $CaCl_2$ in the same buffer for 20 min at 25 °C. The cells were dehydrated in an ascending acetone series and embedded in PolyBed 812 resin. Ultrathin sections were stained with uranyl acetate and lead citrate and examined in a Jeol JEM1011 transmission electron microscope (Tokyo, Japan) (Technological Platform of Electronic Microscopy at Instituto Oswaldo Cruz). Alternatively, dehydrated samples were dried by the critical point method with CO_2, mounted on aluminium stubs, coated with a 20 nm thick gold layer and examined on a Jeol JSM6390LV scanning electron microscope (Tokyo, Japan) (Technological Platform of Electronic Microscopy at Oswaldo Cruz Institute).

2.4.4. Determination of mitochondrial membrane potential and reactive oxygen species production

Trypomastigotes (Y strain, 5×10^6/mL) were treated for 24 h with the selected compounds at concentrations corresponding to half the value of IC_{50}/24 h, IC_{50}/24 h and 2x IC_{50}/24 hand the mitochondrial membrane potential (ΔΨm) and reactive oxygen species (ROS)

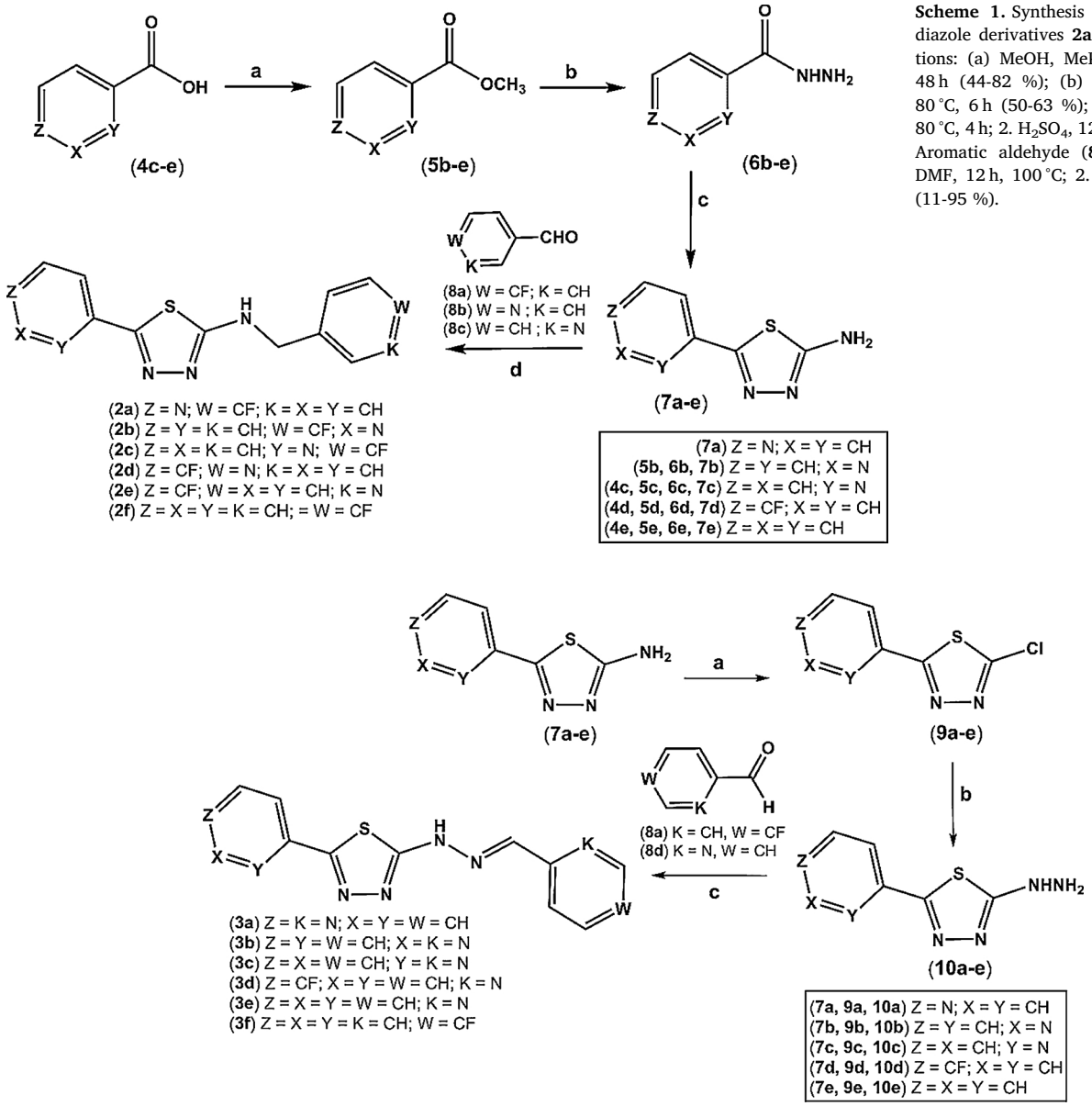

Scheme 1. Synthesis of pyridinyl-1,3,4-thiadiazole derivatives **2a-f**. Reagents and conditions: (a) MeOH, MePh, H_2SO_4 cat., 110 °C, 48 h (44-82 %); (b) NH_2NH_2 80 %, EtOH, 80 °C, 6 h (50-63 %); (c) 1. TMSNCS, EtOH, 80 °C, 4 h; 2. H_2SO_4, 12 h, r.t. (47-69 %); (d) 1. Aromatic aldehyde (**8a-c**), $ZnCl_2$, TMSOAc, DMF, 12 h, 100 °C; 2. $NaBH(OAc)_3$, r.t., 72 h (11-95 %).

Scheme 2. Synthesis of 1,3,4-thiadiazolyl-*N*-arylhydrazone derivatives **3a-f**. Reagents and conditions: (a) 1. $NaNO_2$, HCl, H_2O; 2. $CuCl_2.2H_2O$, 0 °C, 2 h (55–88 %); (b) NH_2NH_2 80 %, EtOH, 80 °C, 2 h (52-81 %); (c) **8a** or **8d**, 10 % HCl (cat.), EtOH, r.t., 4 h (65-90 %).

production were determined. For ΔΨm analysis, the parasites were incubated with 30 μg/mL propidium iodide (PI) plus 50 nM tetramethylrhodamine (TMRE) (Molecular Probes, Carlsbad, USA) for 30 min at 37 °C, using 10 μM carbonyl cyanide 4-(trifluoromethoxy) phenylhydrazone (FCCP) (Sigma-Aldrich) as a control for ΔΨm dissipation. Alterations in TMRE fluorescence were quantified using an index of variation (IV), which was calculated using the equation (MT - MC)/MC, where MT is the median of fluorescence for treated parasites and MC is the median of fluorescence of the control parasites. Negative IV values correspond to depolarization of the mitochondrial membrane. To evaluate ROS generation, labelling with 10 μM dihydroethidium (DHE) (Molecular Probes) for 30 min at 37 °C was performed, using 22 μM antimycin A (AA) (Sigma-Aldrich) as the positive control. The samples were analyzed in a FACSCalibur flow cytometer (Becton Dickinson, CA, USA) (Flow Cytometry and Electron Microscopy Facilities from Instituto Oswaldo Cruz). The Summit program was used for data analysis. A total of 10,000 events were acquired in the region previously established as that of the parasites.

3. Results and discussion

Compounds **2a-f** were obtained by using a 4-stage linear route exploiting classical reactions of functional group interconversions (Scheme 1). Carboxylic acids (**4c-e**) were converted to their respective methyl esters (**5c-e**) in good yield by the Fischer esterification reaction in methanol-toluene with sulfuric acid catalysis [26]. Thereafter, the methyl esters (**5c-e**) were subjected to a hydrazinolysis reaction after treatment with 80 % aqueous hydrazine hydrate in ethanol under reflux to afford the corresponding hydrazides (**6b-e**) in moderate yield [27,39]. Then, equimolar amounts of the hydrazides (**6b-e**) and commercially available trimethylsilyl isothiocyanate (TMSNCS) were maintained under reflux in ethanol to form the *N*-acyl-thiosemicarbazide intermediates, which were next treated with sulfuric acid at room temperature to promote cyclization and subsequent dehydration to furnish the 2-amino-1,3,4-thiadiazoles (**7b-e**) in yields ranging from 47 to 69% [28]. 5-(Pyridin-4-yl)-1,3,4-thiadiazol-2-amine (**7a**) was purchased from Sigma-Aldrich (St. Louis, MO, USA). Finally, the desired 1,3,4-thiadiazole derivatives (**2a-f**) were synthesized in acceptable

yield through reductive amination of the amines (**7a-e**) with the selected aromatic aldehydes (**8a-d**) by using sodium triacetoxyborohydride as the reducing agent after previous formation of the imine intermediate promoted by $ZnCl_2$/TMSOAc in DMF [29].

The synthesis of 1,3,4-thiadiazolyl-*N*-arylhydrazones **3a-g** started from the Sandmeyer reaction of the 1,3,4-thiadiazolylamines (**7a-e**) after treatment with sodium nitrite in hydrochloric acid and water, followed by nucleophilic displacement of the diazonium intermediate with copper chloride to furnish to the corresponding heteroaryl chlorides (**9a-e**) (Scheme 2) [30]. Then, the 1,3,4-thiadiazolyl chlorides (**9a-e**) were subjected to an aromatic nucleophilic substitution reaction with excess hydrazine hydrate in ethanol to give the corresponding heteroarylhydrazines (**10a-e**) in good yield [31]. Finally, the last step for the synthesis of the desired compounds **3a-f** involved the acid-catalyzed condensation between heteroarylhydrazines **11a-e** and the selected aromatic aldehydes (**8a** or **8d**) in ethanol at room temperature [31]. All 1,3,4-thiadiazolyl-*N*-arylhydrazones (**3a-f**) were obtained in high yield. Formation of the hydrazone derivatives as single diastereomers was confirmed due to the presence of a single signal from the hydrogen attached to the imine subunit at approximately 8.1 ppm in the ^{1}H NMR spectra.

It has been reported in the literature that the reaction between hydrazines and pyridine-2-carboxaldehyde (**8d**) leads to the generation of the corresponding hydrazone with the relative *Z* configuration due to the possibility of forming an intramolecular hydrogen bond between the amine hydrogen of the hydrazone group and the pyridine nitrogen, leading to the formation of a stable six-membered ring. Nevertheless, the (*E*)-diastereoisomer would be formed in the minority or would not be formed, since it is not capable of forming this type of intramolecular interaction [40,41] (Scheme 3).

However, although the literature reports the formation of the (*Z*)-diastereomer in the case of 2-pyridinyl-hydrazone, the single diastereoisomer observed among our 1,3,4-thiadiazolyl-*N*-arylhydrazones was characterized as the (*E*)-configuration, since it is known to be the thermodynamic diastereoisomer, with less electronic repulsion that is therefore more stable [32,42].

In order to confirm which diastereomer was obtained, X-ray crystallography studies were conducted. Fortunately, it was possible to obtain adequate resolution of the crystalline structure of compound **3d** (Fig. 4). After observing the ORTEP representation of 1,3,4-thiadiazolyl 2-pyridinylhydrazone **3d**, it was unequivocally confirmed that the diastereoisomer formed presents in the relative (*E*)-configuration.

Some of the 1,3,4-thiadiazole derivatives were subjected to transformation into their corresponding hydrochlorides in order to improve their aqueous solubility and evaluate how this physicochemical behavior could affect their trypanocidal profile. Therefore, compounds **2a**, **2d**, **2e** and **3e** were treated with hydrochloric acid after solubilization in chloroform to furnish the corresponding hydrochlorides **11a**, **11b**, **11c** and **11d** in yields ranging from 62 to 98% (Scheme 4) [32].

The obtained pyridinyl-1,3,4-thiadiazole compounds **2a-f**, **3a-f** and **11a-d** were fully spectroscopically characterized, and their degree of purity was determined by HPLC analysis to be greater than 95 %, which

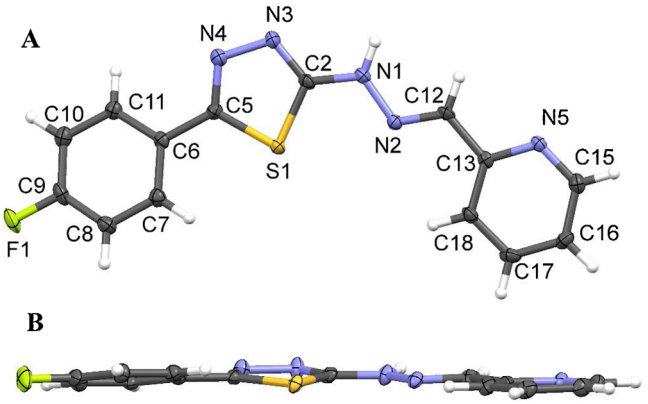

Fig. 4. (A) ORTEP representation of the structure of 1,3,4-thiadiazolyl-*N*-(2-pyridinyl)hydrazine **3d** in the crystalline state. Probability ellipsoids are drawn at the 50 % level. (B) Side-on view of compound **3d**.

is considered adequate for the next step of biological evaluation.

Since *in vitro* assays are strongly influenced by the aqueous solubility of the compound [43], studies were conducted to determine the aqueous solubility of the 1,3,4-thiadiazole derivatives **2a-f** [33]. The results are presented in Table 1. As predicted, compounds having the pyridinyl subunit (**2a-e**) in their structure showed greater aqueous solubility than **2f**, which does not have the azaheterocyclic subunit in its structure. As expected, regioisomers **2a-c** and **2d-e** demonstrated similar aqueous solubility profiles. The aqueous solubilities of the 1,3,4-thiadiazolyl-*N*-arylhydrazone derivatives were similar, and the pyridinyl derivatives **3a-c** showed a greater solubility profile. With respect to compounds **3d** and **3e**, it is relevant to note that insertion of the fluorine atom into **3d** slightly improved the solubility profile of this compound compared to its unsubstituted analog **3e**. Compound **3f**, the only compound in this series in which the pyridinyl subunit is absent, also showed a suitable solubility profile for pharmacological assays.

In general, all 1,3,4-thiadiazole derivatives presented a satisfactory aqueous solubility profile for pharmacological tests [44]. However, as anticipated, we were able to demonstrate an improvement in the aqueous solubility profile of the hydrochlorides **11a-d** of approximately 2- to 4-fold when compared with the solubility of the corresponding free bases (**2a**, **2d**, **2e** and **3e**, respectively) (Table 1). Furthermore, the water solubility profile of the target compounds was similar to that of other previously published 1,3,4-thiadiazole derivatives [45].

It has been reported in the literature that azaheterocyclic fragments are capable of inhibiting the TcCYP51 enzyme; for example, 3-pyridinyl and 4-pyridinyl-containing fragments [19,46]. For this reason, we also chose to test our 1,3,4-thiadiazolylamine intermediates (**7a-e**) in the pharmacological assays.

Initially, we evaluated the effects of the 21 compounds on the infective bloodstream trypomastigotes of the Y strain of *T. cruzi* (Table 2).

Our findings demonstrated that the 2-amino-1,3,4-thiadiazoles **7a-e** did not present an important trypanocidal effect, with IC_{50} values

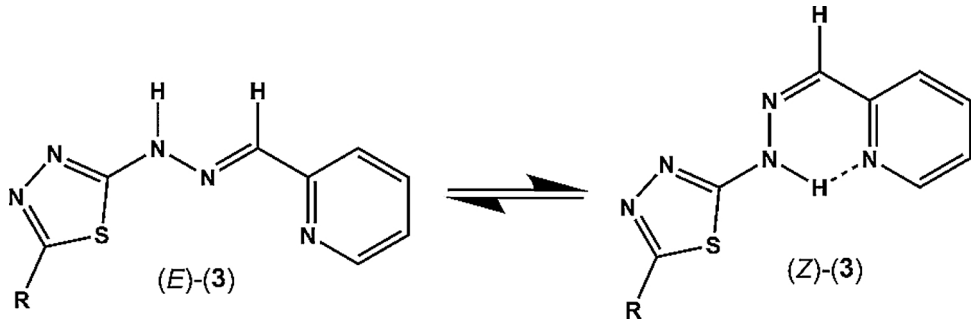

Scheme 3. Representation of the possible (*E*)- and (*Z*)-diastereoisomers of the 1,3,4-thiadiazolyl-*N*-arylhydrazones **3a-f**.

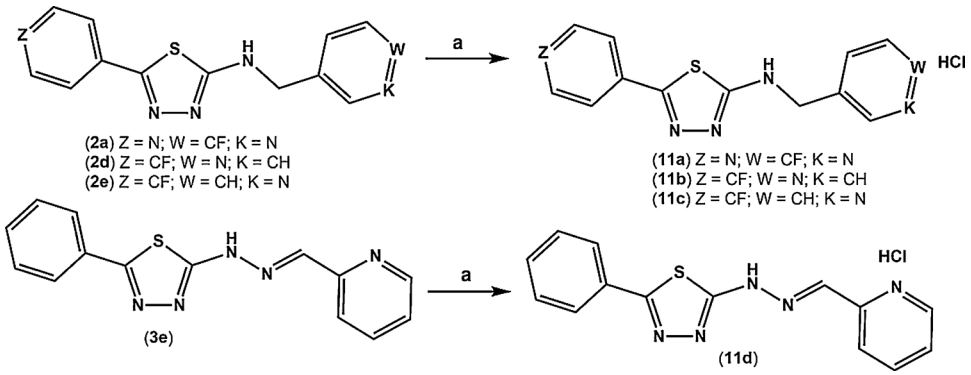

Scheme 4. Synthesis of hydrochlorides **11a-d**. Reagents and conditions: (a) $HCl_{(g)}$, $CHCl_3$, 0 °C, 30 min (62-98 %).

Table 1
Aqueous solubility of the 1,3,4-thiadiazole derivatives **2a-f** and **3a-e** and the hydrochlorides **11a-d**.

Compound	Aqueous solubility[a]	
	mg/mL	μM
2a	1.41×10^{-2}	4.06
2b	1.11×10^{-2}	3.10
2c	1.23×10^{-2}	3.52
2d	1.82×10^{-2}	5.21
2e	2.04×10^{-2}	5.84
2f	3.17×10^{-3}	0.90
3a	1.40×10^{-2}	3.97
3b	1.51×10^{-2}	4.27
3c	5.06×10^{-3}	1.43
3d	2.64×10^{-3}	0.79
3e	1.48×10^{-3}	0.42
3f	1.74×10^{-3}	0.52
11a	6.70×10^{-2}	21.60
11b	5.70×10^{-2}	18.25
11c	9.02×10^{-2}	29.10
11d	1.05×10^{-2}	3.36

[a] Determined by the spectrophotometric method described by Schneider et al. [33] on a scanning UV–vis Femto spectrophotometer (model 800XI).

higher than 200 μM (Table 2). Compound **7a** (4-pyridinyl) showed only modest activity (IC_{50} = 215.0 μM), followed by its ortho-regioisomer **7c** (2-pyridinyl) (IC_{50} = 338.4 μM), while **7b**, with a 3-pyridinyl subunit, was approximately 4-fold less active.

The pyridinyl-1,3,4-thiadiazole derivatives **2a-f** showed a significant increase in trypanocidal activity, with lower IC_{50} values (from 16.6–226.5 μM) relative to their respective amino intermediates **7a-e**, demonstrating that the lipophilic 4-fluorobenzyl unit introduced into the structure contributed considerably to the biological effects. From this series, compound **2a** was the most active, with low toxicity to mammalian macrophages, leading to an excellent selectivity index (SI) of 24.2. Compared to the standard drugs, **2a** was more active than ketoconazole or posaconazole but 2 times less active than benznidazole. It is interesting to note that similar to the results obtained with intermediates **7a-e**, regioisomer **2a** with a 4-pyridinyl subunit showed the highest activity. Thus, despite the classical isosteric relationships between 3-pyridinyl and 2-pyridinyl subunits with the 4-pyridinyl group [20], in the present case, concerning the trypanocidal profile, compounds **2a**, **2b** and **2c** could not be characterized as bioisosteres. Interestingly, although **2a** and **2d** are regioisomers and retroisomers, they showed different activities on trypomastigotes, with **2d** being approximately 14-fold less active. In addition, derivative **2e**, containing a 3-pyridinyl subunit, was more active than **2d** (IC_{50} 24 h of 81.2 μM *versus* 226.5 μM). Thus, despite their high structural similarity, these compounds present different mechanisms of action. It is interesting to note that the pyridinyl group is considered a pharmacophoric group for

Table 2
In vitro activity of the 1,3,4-thiadiazole derivatives on the trypomastigotes of *T. cruzi* (Y strain), cytotoxicity to peritoneal macrophages and selectivity index.

Compound	Bloodstream trypomastigotes[a] IC_{50}/24 h (μM)	Peritoneal macrophages[b] LC_{50}/ 24 h (μM)	SI[c]
7a	215.0 ± 6.9	-[d]	–
7b	832.9 ± 48.1	–	–
7c	338.4 ± 33.0	–	–
7d	340.5 ± 45.0	–	–
7e	> 1000	–	–
2a	16.6 ± 0.9	401.3 ± 41.4	24.2
2b	168.6 ± 25.8	412.8 ± 41.2	2.4
2c	182.9 ± 11.7	391.7 ± 23.7	2.1
2d	226.5 ± 17.6	> 1000	> 4.4
2e	81.2 ± 5.9	119.7 ± 8.8	1.5
2f	190.4 ± 19.7	192.6 ± 5.8	1.0
3a	23.3 ± 5.2	81.4 ± 5.3	3.5
3b	21.6 ± 3.7	102.7 ± 10.6	4.8
3c	9.5 ± 2.3	72.8 ± 2.5	7.7
3d	9.3 ± 3.0	56.1 ± 4.8	6.0
3e	6.7 ± 0.8	443.3 ± 13.7	66.1
3f	52.2 ± 7.1	118.3 ± 13.9	2.3
11a	10.2 ± 2.7	682.0 ± 57.9	66.6
11b	541.3 ± 38.2	206.0 ± 17.5	0.4
11c	170.8 ± 13.7	147.5 ± 22.6	0.9
11d	3.6 ± 0.5	96.7 ± 8.3	26.9
Ketoconazole	118.3 ± 16.1	271.7 ± 37.8	2.3
Posaconazole	> 500	104.6 ± 19.6	< 0.2
Benznidazole	8.8 ± 1.1	> 1000	> 113.6

[a] Treatment for 24 h at 37 °C of the trypomastigotes of *T. cruzi* (Y strain).
[b] Treatment for 24 h at 37 °C of non-infected peritoneal macrophages.
[c] Selectivity index (SI) = LC_{50} of macrophages/IC_{50} of trypomastigotes.
[d] not determined.

the inhibition of TcCYP51; therefore, **2f**, in which this subunit is absent, and **2d**, one of compounds with a 4-pyridinyl group attached in place of the lipophilic anchor D (Fig. 2), both showed only moderate activity against the parasite. This fact suggests that the trypanocidal activity of **2f** and **2d** might not involve TcCYP51 inhibition, and further studies are needed.

To circumvent the solubility issues of **2a-f**, facilitating permeability through biological membranes, hydrochloride analogs were synthesized, resulting in **11a-d**. Interestingly, their activity against *T. cruzi* was inferior to that of the corresponding free bases, with the exception of **11a**, which was more active than **2a** and displayed activity similar to that of Bz and with an SI equal to 66.6 (Table 2).

The series of 1,3,4-thiadiazole-*N*-arylhydrazone derivatives (**3a-f**) showed promising results with excellent IC_{50} values in the range of 6.7–52.2 μM (Table 2). The importance of an adequate water solubility profile for the biological activity is highlighted by the performance of hydrochloride **11d** compared to its free base, **3e** (IC_{50} 3.6 μM *versus* 6.7 μM). Compounds **3a** and **3b** with 4-pyridinyl and 3-pyridinyl subunits,

respectively, showed similar activity and were less active than **3c**, their regioisomer with a 2-pyridinyl subunit. The bioisosteric relationship of **3c-e** with the subunits of 2-pyridinyl, *p*-fluorophenyl and phenyl, respectively, and their similar effects on trypomastigotes suggest that a similar mechanism of action could be involved. In series 3 (**3a-3f**), **3f** presented the lowest trypanocidal activity and is the compound that does not present a 2-pyridinyl subunit compared to **3e** (IC_{50} 52.2 μM *versus* 6.7 μM). Thus, it is clear that for this series, the presence of a 2-pyridinyl subunit linked to the imine functionality of the hydrazone moiety is important for activity against the parasite. In addition, 2-pyridinyl contains a site for metal coordination, so the trypanocidal activity could be related to the coordination of iron ions, for example, which are essential for the survival of *T. cruzi*. The remarkable activity of **3e** can be explained by the insertion of a second nitrogen atom in the side chain, linking the 1,3,4-thiadiazole ring with a 2-pyridinyl group. In this context, it is important to correlate the activity of **3e** with that of 1,3,4-thiadiazole-*N*-arylhydrazones previously reported by our group [31,47], corroborating the pharmacophoric character of the 2-pyridinyl subunit. Compounds **3e** and **11a** demonstrated a low toxicity profile in assays with macrophages, presenting, after 24 h of treatment, LC_{50} values of 443.3 and 682.0 μM, respectively, leading to high selectivity indexes (SI values > 66).

In addition, other compounds structurally similar to those synthesized here, including the thiazolyl-*N*-(2-pyridinyl)hydrazone derivatives described by Da Silva et al. [48], demonstrated excellent trypanocidal action (IC_{50} < 10 μM), with their mode of action interfering with the cell cycle and inducing apoptosis in the parasite, while inhibition of TcCYP51 was not investigated.

The most selective compounds were tested for their cytotoxicity to heart muscle cells, and **2a** (456.5 ± 26.9 μM) and **11a** (423.8 ± 52.7 μM) showed low toxicity to these cells with values above 400 μM after 24 h of treatment, while the corresponding values for **3e** and **11d** were 29.9 ± 4.3 and 120.9 ± 2.9 μM.

Whereas compound **3e** exhibited low selectivity in HMC and **11d** had the lowest aqueous solubility, only compound **2a** and its hydrochloride **11a** were selected for evaluation of their activity against intracellular amastigotes. A dose- (20–80 μM) and time- (24 and 48 h) dependent effect on the proliferation of intracellular amastigotes was observed for both compounds, with SI values between 3.4 and 11.0 (Fig. 5).

Light microscopy analysis illustrated the results obtained for the inhibition of amastigote proliferation by pyridinyl-1,3,4-thiadiazole derivative **2a** and its hydrochloride **11a** (Fig. 6). Both compounds, even at the highest concentration used, did not interfere with the contractibility and cellular organization of the cardiac cells.

The ultrastructural alterations induced by compound **11a** in the *T. cruzi* trypomastigote forms were investigated by electron microscopy using the concentration corresponding to its IC_{50}/24 h value (10 μM). TEM analysis revealed that **11a** led to blebbing of the plasma membrane and the appearance of atypical vacuoles (Fig. 7**B–E**). The most prominent phenotypic changes observed in the treated parasites was the alteration in the shape of the kinetoplast, presenting with a rod-like appearance, similar to amastigote kinetoplasts (Fig. 7**B–E**). Untreated parasites exhibited a typical morphology with characteristic rounded kinetoplasts (Fig. 7**A** (K)).

Corroborating the TEM data, which revealed parasites with alterations in the kinetoplast appearance and probably alteration in the form of the parasite, trypomastigotes treated with **11a** and observed by SEM also displayed a rounded body. SEM analysis revealed that **11a** induced severe morphological changes in trypomastigotes (Fig. 8), with rounding of the parasite's body and flagellum shortening (Fig. 8**B–D**) compared to untreated cells (Fig. 8A). These alterations, such as surface shrinkage, induced by this derivative may indicate destabilization of cytoskeleton components or microtubule-associated proteins [49].

Veiga-Santos and coworkers [50] observed that treatment of epimastigote forms of *T. cruzi* with posaconazole led to intense alteration of the cell shape, similar to that observed by our group in the organization of the Golgi complex, leading to the formation of autophagic vacuoles and the loss of kDNA compaction. Treating L. *amazonensis* promastigotes with posaconazole, De Macedo-Silva et al. [51] observed retraction of the parasite's body and several alterations in the mitochondrion-kinetoplast complex, including images suggesting decompaction of the kinetoplast, the presence of cytoplasmic vacuoles containing vesicles and profound changes in the plasma membrane. It was further described by TEM that treatment for 48 h with ketoconazole in epimastigotes of *T. cruzi* also induced alterations in the membrane, mitochondrion and reservosomes [52]. Both studies, with different trypanosomatids treated with posaconazole, showed alterations in the shape of the kinetoplast and plasma membrane, as well as the presence of cytoplasmatic vacuoles, as observed by our group after treatment of

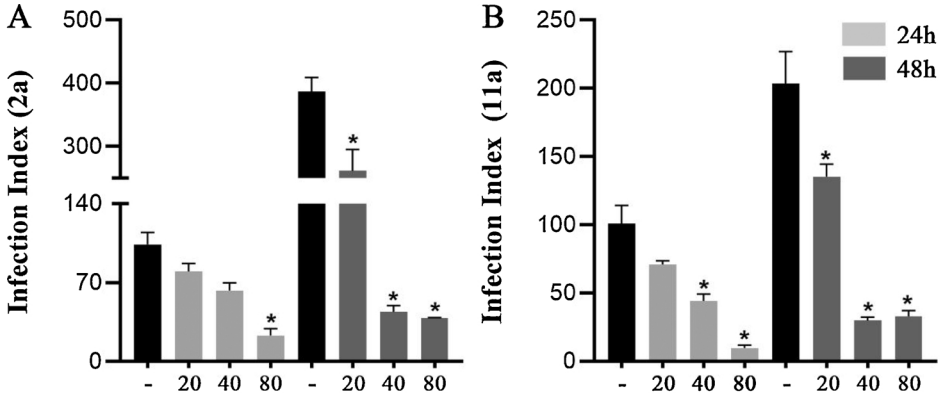

Fig. 5. Infection indexes for *T. cruzi*-infected HMCs after treatment for 24 and 48 h with (A) 20-80 μM **2a** and (B) its hydrochloride **11a**. HMCs were infected with bloodstream trypomastigotes (MOI 10:1), and after 24 h of infection, the cells were treated with **2a** or **11a** for 24 or 48 h. The infection index corresponds to the number of parasites/100 cells, obtained by the percent of infection multiplied by the number of parasites/infected cell, and the IC_{50} values (Table) with 50 % inhibition of this parameter. The selectivity index (SI) corresponds to the ratio between the LC_{50} for HMCs and the IC_{50} for the infection index. Asterisks indicate significant differences in relation to the untreated control group ($p \leq 0.05$) by ANOVA followed by Bonferroni's posttest.

	2a			11a		
	IC_{50} (μM)	LC_{50} (μM)	SI	IC_{50} (μM)	LC_{50} (μM)	SI
24 h	63.4 ±7.7	456.5±26.9	7.2	42.7±5.1	423.8±52.7	9.9
48 h	28.3±3.8	95.8±5.9	3.4	30.4±3.3	333.6±51.0	11.0

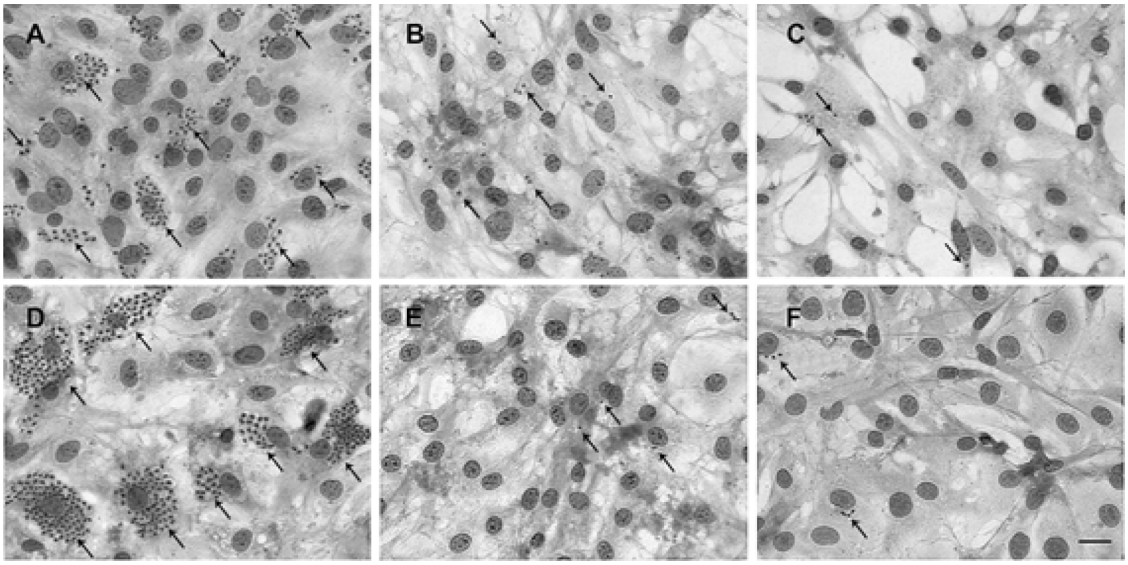

Fig. 6. Effect of **2a** and **11a** on HMCs infected with *T. cruzi* (Y strain) after 24 and 48 h. (A) Control/24 h; (B) 80 μM **2a**/24 h; (C) 80 μM **11a**/24 h; (D) control/48 h; (E) 80 μM **2a**/48 h; (F) 80 μM **11a**/48 h. Bars = 20 μm. Black arrows indicate intracellular parasites.

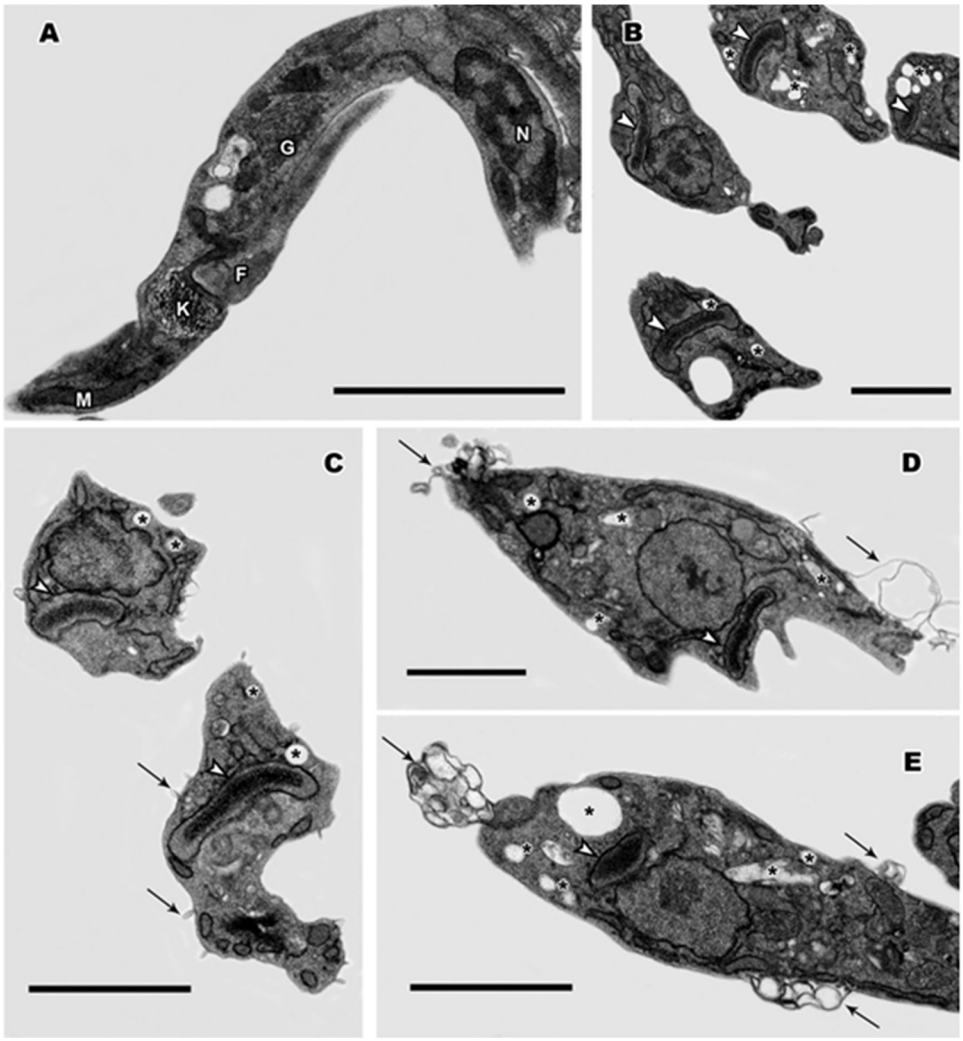

Fig. 7. Transmission electron microscopy analysis of *T. cruzi* trypomastigotes. (A) Untreated trypomastigotes showing normal ultrastructural aspects and presenting typical morphologies of the mitochondria (M), kinetoplast (K), flagellum (F), nucleus (N) and Golgi apparatus (G). (B-E) Trypomastigotes treated with IC_{50}/24 h = 10 μM **11a** showing blebs in the plasma membrane (thin black arrows), alterations in the shape of the kinetoplast, presenting with a rod-like appearance, similar to the amastigote kinetoplast (white arrowheads) and an increase in the number of cytoplasmic vacuoles (black asterisk). Bars = 2 μm.

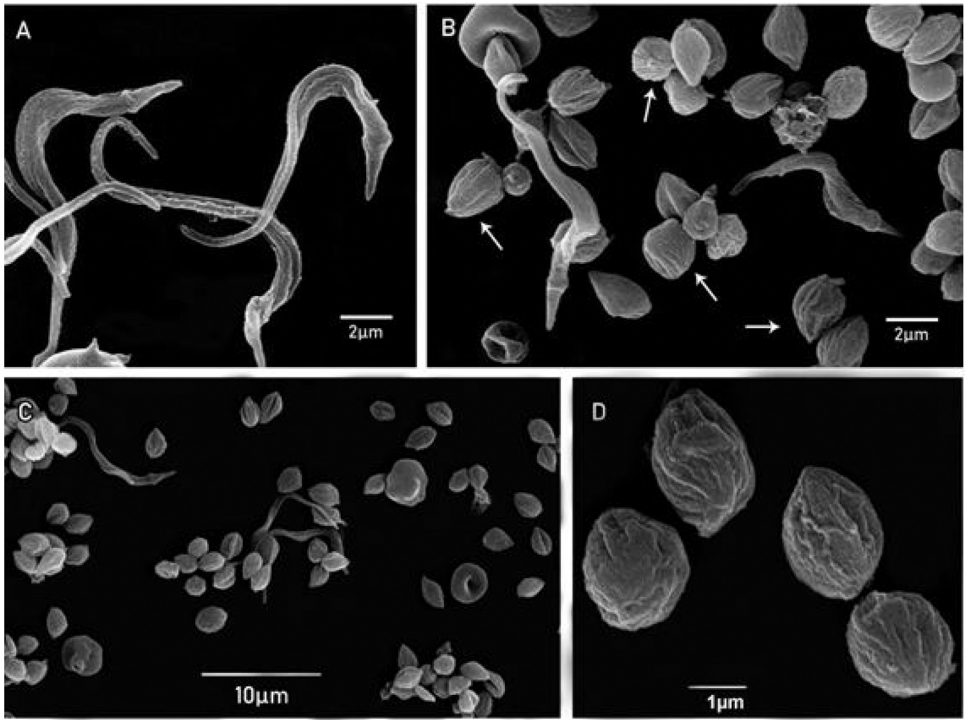

Fig. 8. Scanning electron microscopy analysis of trypomastigotes: (**A**) Untreated trypomastigotes with typical morphology; an elongated shape and flagellum located laterally in the posterior region of the parasite; (**B-D**) trypomastigotes treated with 10 μM **11a** for 24 h showing the retraction and rounding of the parasite body and loss of the flagellar structure (thin arrow).

Table 3
Flow cytometry analysis of the mitochondrial membrane, generation of ROS and plasma membrane integrity in *T. cruzi* trypomastigotes treated with 11a for 24 h.

	μM	IV TMRE	% TMRE +	% DHE +	% PI +
Control	–	1.00[a]	90.4 ± 5.8[b]	15.3 ± 8.2	4.2 ± 2.0
11a	**5**	1.15	89.7 ± 6.2	6.7 ± 5.2	4.2 ± 2.9
	10	1.13	88.6 ± 5.8	8.1 ± 3.8	3.3 ± 1.6
	15	1.06	80.4 ± 10.1	9.9 ± 4.1	6.0 ± 3.6

[a] IV = (MT–MC)/MC, where MT corresponds to the median fluorescence for treated parasites and MC corresponds to that of control parasites.
[b] Mean ± standard deviation of three independent experiments.

trypomastigotes with **11a**.

Following the ultrastructural analysis of **11a**, the mitochondrial membrane potential, generation of reactive oxygen species and plasma membrane integrity were evaluated by flow cytometry. Our results suggest that treatment with **11a** does not alter these parameters even at concentrations corresponding to 2× IC_{50}/24 h (Table 3). Previous studies indicate that sterol biosynthesis inhibitors are able to induce alterations in mitochondrial structure and function, as this organelle has a special requirement for sterols [52,53]. De Macedo-Silva and coworkers [51] reported that posaconazole treatment in L. *amazonensis* promastigotes compromised plasma membrane integrity after 48 h of treatment. In another study with posaconazole-treated L. *amazonensis*, the De Macedo-Silva group showed that this drug was able to induce an increase in ROS production and collapse the mitochondrial transmembrane electric potential [54]. Additionally, treatment with ketoconazole in *T. cruzi* epimastigotes also induced time-dependent mitochondrial depolarization and a loss of plasma membrane integrity [55]. This finding suggests that these phenotypic alterations caused by inhibitors of sterol biosynthesis could be generated only with longer treatment times, unlike the trypomastigote treatment time in these studies.

4. Conclusion

Fortunately, all 1,3,4-thiadiazole derivatives presented activity against the trypomastigote form of *T. cruzi*. The IC_{50} values of the amino-substituted 1,3,4-thiadiazole derivatives (**2a-f**) ranged from 16.6–226.5 μM, and the values for the 1,3,4-thiadiazole-*N*-arylhydrazone series (**3a-f**) ranged from 6.7–52.2 μM. Regarding the derivatives **3a-f**, it was evident that the 2-pyridinyl fragment bound to the imine subunit of the hydrazine moiety presents pharmacophoric behavior for trypanocidal activity.

Four hydrochlorides (**11a-d**) were also synthesized and, as planned, presented a better aqueous solubility profile than their corresponding free bases. Considering the potencies, two of these hydrochlorides, *i.e.*, **11b** and **11c**, showed a significant decrease in trypanocidal action, while the other two, **11a** and **11d**, potentiated the trypanocidal action of their respective free bases (**2a** and **3e**, respectively).

The 1,3,4-thiadiazole prototypes **2a** and **11a** presented remarkable trypanocidal action on trypomastigotes and excellent selectivity indexes. Additionally, **2a** and **11a** demonstrated trypanocidal effects on the amastigote form of *T. cruzi*. Moreover, the corresponding hydrochloride **11a** presented the most promising profile, producing phenotypic changes similar to those promoted by treatment with the standard drug posaconazole. For this reason, 1,3,4-thiadiazole derivative **11a** could be considered a good prototype for the development of drug candidates for Chagas disease therapy.

Funding source

None.

Declaration of Competing Interest

None.

Acknowledgments

The authors thank Dr. Solange Lisboa de Castro for critical reading of the manuscript. We also thank the Technological Platform of Electronic Microscopy and Flow Cytometry and Electron Microscopy Facilities at Instituto Oswaldo Cruz. The authors are also grateful to Fundação de Amparo à Pesquisa do Rio de Janeiro (FAPERJ, BR),

Coordenação de Aperfeiçoamento de Pessoal de Nivel Superior (CAPES, BR), Conselho Nacional de Desenvolvimento Científico e Tecnológico (CNPq, BR) and Fundação Oswaldo Cruz (FIOCRUZ, BR) for financial support and fellowships.

Appendix A. Supplementary data

Supplementary material related to this article can be found, in the online version, at doi:https://doi.org/10.1016/j.biopha.2020.110162.

References

[1] C. Chagas, Mem. Inst. Oswaldo Cruz 1 (1909) 159–218, https://doi.org/10.1590/S0074-02761909000200008.

[2] WHO Neglected Tropical Diseases, (2020) (Accessed June 27, 2019), https://www.who.int/neglected_diseases/en/.

[3] J.R. Coura, S. L De Castro, Mem. Inst. Oswaldo Cruz 97 (2002) 3–24, https://doi.org/10.1590/S0074-02762002000100001.

[4] (a) J.R. Coura, J. Borges-Pereira, Mem. Inst. Oswaldo Cruz 106 (2011) 641–645, https://doi.org/10.1590/S0074-02762011000600001;
(b) J.C. Dias, A.N. Ramos Jr., E.D. Gontijo, A. Luquetti, M.A. Shikanai-Yasuda, J.R. Coura, R.M. Torres, J.R. Melo, E.A. Almeida, W. Oliveira Jr., A.C. Silveira, J.M. Rezende, F.S. Pinto, A.W. Ferreira, A. Rassi, A.A. Fragata-Filho, A.S. Sousa, D. Correia-Filho, A.M. Jansen, G.M. Andrade, C.F. Britto, A.Y. Pinto, A. Rassi-Jr, D.E. Campos, F. Abad-Franch, S.E. Santos, E. Chiari, A.M. Hasslocher-Moreno, E.F. Moreira, D.S. Marques, E.L. Silva, J.A. Marin-Neto, L.M. Galvão, S.S. Xavier, S.A. Valente, N.B. Carvalho, A.V. Cardoso, R.A. Silva, V.M. Costa, S.M. Vivaldini, S.M. Oliveira, V.D. Valente, L.M. Lima, R.V. Alves, Epidemiol. Serv. Saúde 25 (2016) 7–86, https://doi.org/10.5123/S1679-49742016000500002.

[5] K. Salomão, R.F.S. Menna-Barreto, S. L De Castro, Curr. Top. Med. Chem. 16 (2016) 2266–2289, https://doi.org/10.2174/1568026616666160413125049.

[6] (a) M. Kaiser, M. P.Mäser, L. P.Tadoori, J.R. Ioset, R. Brun, PLoS One 10 (2015) e0135556, , https://doi.org/10.1371/journal.pone.0135556;
K. Salomão, S. L. De Castro. Leon L & Torres-Santos EC, Nova Science Publishers, NY, 2017, pp. 181-226.

[7] J.A. Urbina, Mem. Inst. Oswaldo Cruz 104 (Suppl. 1) (2009) 311–318, https://doi.org/10.1590/s0074-02762009000900041.

[8] G.I. Lepesheva, T.Y. Hargrove, S. Anderson, Y. Kleshchenko, V. Furtak, Z. Wawrzak, F.M.R. Waterman, J. Biol. Chem. 285 (2010) 25582–25590, https://doi.org/10.1074/jbc.M110.133215.

[9] X. Yu, V. Cojocaru, G. Mustafa, O. M.Salo-Ahen, G.I. Lepesheva, R.C. Wade, J. Mol. Recognit. 28 (2015) 59–73, https://doi.org/10.1002/jmr.2412.

[10] G.I. Lepesheva, F. Villalta, M.R. Waterman, Adv. Parasitol. 75 (2011) 65–87, https://doi.org/10.1016/B978-0-12-385863-4.00004-6.

[11] F.S. Buckner, J.A. Urbina, Int. J. Parasitol.-Drug. 2 (2012) 236–242, https://doi.org/10.1016/j.ijpddr.2011.12.002.

[12] S.S. Gunatilleke, C.M. Calvet, J.B. Johnston, C.K. Chen, G. Erenburg, J. Gut, J.C. Engel, K.K. Ang, J. Mulvaney, S. Chen, M.R. Arkin, J.H. McKerrow, L.M. Podust, PLoS Negl. Trop. Dis. 6 (2012) e1736, https://doi.org/10.1371/journal.pntd.0001736.

[13] R.F. Menna-Barreto, S.L. De Castro, Curr. Top. Med. Chem. 17 (2017) 1212–1234, https://doi.org/10.2174/1568026616666161025161858.

[14] D.J. Leaver, Molecules 23 (2018) E1753, https://doi.org/10.3390/molecules23071753.

[15] I. Molina, J.G. Prat, F. Salvador, B. Treviño, E. Sulleiro, N. Serre, D. Pou, S. Roure, J. Cabezos, L. Valerio, A. Blanco-Grau, A. Sánchez-Montalvá, X. Vidal, A. Pahissa, New Engl. J. Med. 370 (2014) 1899–1907, https://doi.org/10.1056/NEJMoa1313122.

[16] F. Torrico, J. Gascon, L. Ortiz, L.C. Alonso-Veja, M.J. Pinazo, A. Schijman, I.C. Almeida, F. Alves, N. Strub-Wourgaft, I. Ribeiro, Lancet Infect. Dis. 18 (2018) 419–430, https://doi.org/10.1016/S1473-3099(17)30538-8.

[17] DNDi, (2020) https://www.dndial.org/wp-content/uploads/2019/03/2page_BenditatStudyOverview_ENG.pdf.

[18] J.Y. Choi, L.M. Podust, W.R. Roush, Chem. Rev. 114 (2014) 11242–11271, https://doi.org/10.1021/cr5003134.

[19] T.Y. Hargrove, Z. Wawrzak, P.W. Alexander, J.H. Chaplin, M. Keenan, S.A. Charman, C.J. Perez, M.R. Waterman, E. Chatelain, G.I. Lepesheva, J. Biol. Chem. 288 (2013) 31602–31615, https://doi.org/10.1074/jbc.M113.497990.

[20] L.M. Lima, E.J. Barreiro, Curr. Med. Chem. 12 (2005) 23–49, https://doi.org/10.2174/0929867053363540.

[21] G. Nagendra, R.S. Lamani, N. Narendra, V.V. Sureshbabu, Tetrahedron Lett. 51 (2010) 6338–6341, https://doi.org/10.1016/j.tetlet.2010.09.122.

[22] Y. Hu, C.-Y. Li, X.-M. Wang, Y.-H. Yang, H.-L. Zhu, Chem. Rev. 114 (2014) 5572–5610, https://doi.org/10.1021/cr400131u.

[23] E.J. Barreiro, C.A.M. Fraga, Química Medicinal: As Bases Moleculares da Ação dos Fármacos, 3. ed., Porto Alegre: Artmed, 2015 590p.

[24] K. Ji, C. Lee, B.G. Janesko, E.E. Simanek, Mol. Pharm. 12 (2015) 2924–2927, https://doi.org/10.1021/acs.molpharmaceut.5b00205.

[25] S. Rollas, Ş.G. Küçükgüzel, Molecules 12 (2007) 1910–1939, https://doi.org/10.3390/12081910.

[26] R. Moszczynski-Petkowski, J. Majer, M. Borkowska, L. Bojarski, S. Janowska, M. Matłoka, F. Stefaniak, D. Smuga, K. Bazydło, K. Dubiel, M. Wieczorek, Eur. J. Med. Chem. 155 (2018) 96–106, https://doi.org/10.1016/j.ejmech.2018.05.043.

[27] P.C. Lima, C.L.M. Lima, M.K.C. Da Silva, P.H. Léda, A.L.P. De Miranda, C.A.M. Fraga, E.J. Barreiro, Eur. J. Med. Chem. 35 (2000) 187–203, https://doi.org/10.1016/s0223-5234(00)00120-3.

[28] D.R. Guda, H.M. Cho, M.E. Lee, RSC Adv. 3 (2013) 7684–7687, https://doi.org/10.1039/C3RA41044G.

[29] A.V. Bogolubsky, Y. S.Moroz, S.E. Pipko, D.M. Panov, A.I. Konovets, R. Doroschuk, A. Tolmachev, Synthesis 46 (2014) 1765–1772, https://doi.org/10.1055/s-0033-1341226.

[30] C. Prouillac, P. Vicendo, J.C. Garrigues, R. Poteau, G. Rima, Free Rad. Biol. Med. 46 (2009) 1139–1148, https://doi.org/10.1016/j.freeradbiomed.2009.01.016.

[31] S.A. Carvalho, E.F. da Silva, R.M. Santa-Rita, S.L. de Castro, C.A.M. Fraga, Bioorg. Med. Chem. Lett. 14 (2004) 5967–5970, https://doi.org/10.1016/j.bmcl.2004.10.007.

[32] I.A. Guedes, R.H.C.N. Freitas, N.M. Cordeiro, T.S. Do Nascimento, T.S. Valerio, et al., ChemMedChem 11 (2016) 234–244, https://doi.org/10.1002/cmdc.201500266.

[33] P. Schneider, M. Hosseiny, M. Szczotka, V. Jordan, K. Schlitter, Phytochem. Lett. 2 (2009) 85–87, https://doi.org/10.1016/j.phytol.2008.12.004.

[34] K. Salomão, E.M. De Souza, S.A. Carvalho, E.F. Da Silva, C.A.M. Fraga, H.S. Barbosa, S.L. De Castro, Antimicrob. Agents Chemother. 54 (2010) 2023–2031, https://doi.org/10.1128/AAC.01241-09.

[35] L.H.P. Silva, V. Nussenszweig, Folia Clin. Biol. 20 (1953) 191–207.

[36] M.N. Meirelles, T.C. De Araujo-Jorge, C.F. Miranda, W. De Souza, H.S. Barbosa, Eur. J. Cell Biol. 41 (1986) 198–206.

[37] D.G.J. Batista, M.M. Batista, G.M. Oliveira, P. Borges, J. Lannes-Vieira, C.C. Britto, A. Junqueira, M.M. Lima, A.J. Romanha, P.A. Sales-Junior, C.E. Stephens, D.W. Boykin, M.N.C. Soeiro, Antimicrob. Agents Chemother. 54 (2010) 2940–2952, https://doi.org/10.1128/AAC.01617-09.

[38] (a) G.A.M. Jardim, T.L. Silva, M.O.F. Goulart, C.A. De Simone, J.M.C. Barbosa, K. Salomão, S.L. De Castro, J.F. Bower, E.N. Da Silva-Júnior, Eur. J. Med. Chem. 136 (2017) 406–419, https://doi.org/10.1016/j.ejmech.2017.05.011;
(b) M.N. Meirelles, T.C. De Araujo-Jorge, C.F. Miranda, W. De Souza, H.S. Barbosa, Eur. J. Cell Biol. 41 (1986) 198–206.

[39] I.G. Ribeiro, K.C.M. Da Silva, S.C. Parrinil, A.L.P. De Miranda, C.A.M. Fraga, E.J. Barreiro, Eur. J. Med. Chem. 33 (1998) 225–235, https://doi.org/10.1016/S0223-5234(98)80012-3.

[40] G. Palla, G. Prediere, C. Vignalli, Gazz. Chim. Ital. 112 (1982) 339–341.

[41] G. Palla, G. Prediere, P. Domiano, Tetrahedron 42 (1986) 3649–3654, https://doi.org/10.1016/S0040-4020(01)87332-4.

[42] N.M. Cordeiro, R.H.C.N. Freitas, C.A.M. Fraga, P.D. Fernandes, PLoS One 11 (2016) e0156271, , https://doi.org/10.1371/journal.pone.0156271.

[43] J.B. Dressman, B.C. Reppas, Eur. J. Pharm. Sci. 11 (2000) 73–80, https://doi.org/10.1016/s0928-0987(00)00181-0.

[44] K.T. Savjani, A.K. Gajjar, J.K. Savjani, ISRN Pharm. (2012) 195727, , https://doi.org/10.5402/2012/195727.

[45] A. Brai, S. Ronzini, V. Riva, L. Botta, C. Zamperini, M. Borgini, C.I. Trivisani, A. Garbelli, C. Pennisi, A. Boccuto, F. Saladini, M. Zazzi, G. Maga, M. Botta, Molecules 24 (2019) 3988, https://doi.org/10.3390/molecules24213988.

[46] C.M. Calvet, D.F. Vieira, J.Y. Choi, D. Kellar, M.D. Cameron, J.L. Siqueira-Neto, J. Gut, J.B. Johnston, L. Lin, S. Khan, J.H. McKerrow, W.R. Roush, L.M. Podust, J. Med. Chem. 57 (2014) 6989–7005, https://doi.org/10.1021/jm500448u.

[47] S.A. Carvalho, F.A.S. Lopes, K. Salomão, N.C. Romeiro, S.M.V.S. Wardell, S.L. De Castro, E.F. Da Silva, C.A.M. Fraga, Bioorg. Med. Chem. 16 (2008) 413–421, https://doi.org/10.1016/j.bmc.2007.09.027.

[48] E.B. da Silva, D.A.O. Silva, A.R. Oliveira, C.H.S. Mendes, T.A.R. Santos, A.C. Da Silva, M.C. De Castro, R.S. Ferreira, D.R. Moreira, M.V. Cardoso, C.A. De Simone, V.R. Pereira, A.C. Leite, Eur. J. Med. Chem. 130 (2017) 39–50, https://doi.org/10.1016/j.ejmech.2017.02.026.

[49] T. Souto-Padrón, T.U. de Carvalho, E. Chiari, W. De Souza, Acta Trop. 1 (1984) 215–225.

[50] P. Veiga-Santos, E.S. Barrias, J.F.C. Santos, T.L.B. Moreira, T.M.U. de Carvalho, Julio A. Urbina, W. de Souza, Int. J. Antimicrob. Agents 40 (2012) 61–71, https://doi.org/10.1016/j.ijantimicag.2012.03.009.

[51] S.T. de Macedo-Silva, J.A. Urbina, W. de Souza, J.C.F. Rodrigues, PLoS One 8 (2013) e83247, , https://doi.org/10.1371/journal.pone.0083247.

[52] R.L. Kessler, M.J. Soares, C.M. Probst, M.A. Krieger, PLoS One 8 (2013) e55497, , https://doi.org/10.1371/journal.pone.0055497.

[53] I.V. Palmié-Peixoto, M.R. Rocha, J.A. Urbina, W. de Souza, M. Einicker-Lamas, M.C.M. Motta, FEMS Microbiol. Lett. 255 (2006) 33–42, https://doi.org/10.1111/j.1574-6968.2005.00056.x.

[54] S.T. de Macedo-Silva, G. Visbal, J.A. Urbina, W. de Souza, J.C.F. Rodrigues, Antimicrob. Agents Chemother. 59 (2015) 6402–6418, https://doi.org/10.1128/AAC.01150-15.

[55] R.M. Santa-Rita, R. Lira, H.S. Barbosa, J.A. Urbina, S.L. De Castro, J. Antimicrob. Chemother. 55 (2005) 780–784, https://doi.org/10.1093/jac/dki087.